II.1

Complete Seismic-Ray Tracing in Three-Dimensional Structures

V. ČERVENÝ
Institute of Geophysics, Charles University, Praha, Czechoslovakia

L. KLIMEŠ
Institute of Geology and Geotechnics, Czechoslovak Academy of Sciences, Praha, Czechoslovakia

I. PŠENČÍK
Geophysical Institute, Czechoslovak Academy of Sciences, Praha, Czechoslovakia

1 INTRODUCTION

The ray method and its extensions have recently found many applications in the numerical modelling and interpretation of seismic wavefields in complex two- and three-dimensional structures. The basic and numerically most time-consuming step in the application of the ray method consists in the computation of rays. Ray tracing plays an important role not only in the ray method itself but also in its more sophisticated extensions. In standard ray tracing only the ray trajectory, travel times and slowness vectors along the ray are determined. The components of the slowness vector also represent the first partial derivatives of the travel-time field with respect to spatial coordinates. All these quantities are very important in certain seismological applications, but are not sufficient to solve many other seismological problems.

It is, however, possible to slightly extend the ray-tracing algorithm and to evaluate many other quantities of great seismological importance along the ray (both in the numerical modelling of seismic wavefields and in the solution of inverse problems). Among other things, the ray propagator

SEISMOLOGICAL ALGORITHMS
ISBN 0-12-220770-X

matrix can be computed by means of so-called dynamic ray tracing. If the ray propagator matrix is known then many important seismological problems in the vicinity of the evaluated ray may be solved analytically, without additional numerical ray tracing. It is also not difficult to evaluate several other quantities along the ray; these can then be used for a simple computation of the ray amplitudes.

In this chapter, we propose and describe in detail an algorithm for *complete ray tracing*. Complete ray tracing consists of (a) standard ray tracing, (b) dynamic ray tracing (computation of the ray propagator matrix) and (c) evaluation of the components of the reduced vectorial complex-valued amplitudes. The algorithm for complete ray tracing is, of course, more involved than the algorithm for standard ray tracing, but numerically complete ray tracing is not much more time-consuming than ray tracing itself. Complete ray tracing considerably extends the possibilities and applicability of standard ray tracing and is sure to find an important place in most program packages designed for the numerical modelling of high-frequency (HF) seismic body wavefields in complex structures and for the solution of seismic inverse problems.

In the algorithm for complete ray tracing, a three-dimensional (3D) laterally varying isotropic block structure, specified in an arbitrary curvilinear coordinate system, is considered. The description of the model is rather general, and in principle it follows the proposals of Gjøystdal *et al.* (1985). The proposed algorithms allow us to consider virtually any type of seismic HF body wave propagating in such a medium.

The algorithms described in this chapter are not always simple and straightforward. It would, however, increase the length of the chapter inordinately to try to derive here all the required equations and to explain all steps in the algorithm from the seismological point of view. The most complete and consistent theory of complete ray tracing in general 3D layered media can be found in Červený (1985a). In the latter work Cartesian coordinates are used, but the algorithms proposed here are written for an arbitrary curvilinear coordinate system. For this reason, all the equations required in the algorithms are presented in complete form, even though their derivations are not given.

For specific seismological problems, it would be computationally more efficient to use some simplified algorithms. This chapter considers only the most general case; simplifications for special cases are left to the reader.

The structure of the algorithm for complete ray tracing proposed here is as follows. The full problem of complete ray tracing is divided into several, more or less independent algorithms. This chapter consists of a

detailed description of these algorithms. The system of algorithms is full and sufficient for the complete ray tracing of a single ray in 3D structures. The results of complete ray tracing are assumed to be stored in output files, which may be used later in various problems of seismological importance.

In the derivation of the algorithm for complete ray tracing presented here we have profited a great deal from our long experience with numerical modelling of HF seismic wavefields in complex 2D and 3D structures and with 2D and 3D seismic-ray packages. This has allowed us to propose some more general and more efficient algorithms and a more convenient structure of the whole program. This chapter describes algorithms for such a new program.

In the proposed algorithm only a single ray of a selected elementary wave, specified by proper *initial conditions,* is considered. The two-point ray tracing problem is discussed only briefly, and not in full generality, for paraxial rays only. The results of complete ray tracing offer the possibility of solving the two-point ray-tracing problem for paraxial rays analytically (see Section 7.12). The general solution of the two-point ray-tracing problem is not included in the complete ray-tracing algorithm, even though the results of complete ray tracing may be useful in this problem. Likewise, the results of complete ray tracing are of basic importance in the computation of synthetic seismograms, synthetic frequency responses, elastodynamic Green functions etc. Such computations, however, require consideration of rays of various elementary waves. Thus, to perform them the user must supply his or her own routine in which the complete ray-tracing routines will be used successively for individual rays of the elementary waves. For the reader's convenience, the full equations for such computations are given in Sections 7.20–7.22.

In complete ray tracing only standard (zeroth-order) ray approximations are used to evaluate the amplitudes. Complete ray tracing, however, also yields quantities that are very useful and important in the evaluation of HF seismic wavefields in singular regions (vicinity of caustics, critical regions etc.) and in the evaluation of various diffracted waves. Such computations may be performed by programs not described here, but involving the results of complete ray tracing. Similarly, complete ray tracing is a basic routine in the evaluation of Gaussian beams and in the computation of HF seismic body wavefields by summation of Gaussian beams, by the extended WKBJ method, by the Maslov method, and so on. A detailed treatment of this subject is beyond the scope of this chapter.

Most equations in this chapter are written in component notation.

Capital-letter indices ($I, J, K, A, B, \ldots$) take values 1 and 2, lower-case indices ($i, j, k, a, b, \ldots$) take values 1, 2, 3, and Greek lower-case indices ($\alpha, \beta, \gamma, \ldots$) take values 1, 2, 3, 4. The Einstein summation convention is used, with respect to both repeated subscripts and superscripts.

Together with component notation, matrix notation is also used. Matrices are denoted by boldface sans serif letters. In order to distinguish between 2×2 and 3×3 matrices, the latter are denoted with a circumflex above the letter. If the same boldface letter is used for 2×2 and 3×3 matrices with and without the circumflex (e.g. $\mathbf{M}$ and $\hat{\mathbf{M}}$) then the matrix without the circumflex ($\mathbf{M}$) is the 2×2 upper left-hand minor of the 3×3 matrix with a circumflex ($\hat{\mathbf{M}}$). Thus M_{IJ} are components of $\mathbf{M}$, and M_{ij} those of $\hat{\mathbf{M}}$.

2 COORDINATE SYSTEM

2.1 Metric tensor and Christoffel symbols

We consider general right-handed curvilinear coordinates (x^1, x^2, x^3). The local properties of the coordinate system are described by the covariant components $G_{ij} = G_{ij}(x^k)$ or by the contravariant components $G^{ij} = G^{ij}(x^k)$, $i, j, k = 1, 2, 3$, of the metric tensor and by the Christoffel symbols

$$\Gamma^k_{ij} = \tfrac{1}{2} G^{kl}(G_{il,j} + G_{jl,i} - G_{ij,l}). \tag{2.1}$$

The metric tensor is symmetric and generally has six independent components. The covariant G_{ij} and contravariant G^{ij} components of the metric tensor are related by

$$G^{ij} G_{ik} = \delta^j_k,$$

where the mixed co- and contravariant Kronecker delta δ^i_j is equal to 1 for $i = j$ and 0 otherwise. The square of the infinitesimal length $\mathrm{d}s$ can be expressed in terms of the metric tensor as follows:

$$\mathrm{d}s^2 = G_{ij}\, \mathrm{d}x^i\, \mathrm{d}x^j.$$

There are generally 18 independent Christoffel symbols.

The routine designed for the determination of the metric tensor and of Christoffel symbols at any point is here called METRIC.

2.2 Examples of the most important coordinate systems

2.2.1 Cartesian coordinate system

In Cartesian coordinates,

$$G_{ij} = \delta_{ij}, \qquad G^{ij} = \delta^{ij}, \tag{2.2}$$

$$\Gamma^k_{ij} = 0. \tag{2.3}$$

Here the covariant and contravariant forms of the Kronecker delta δ_{ij} and δ^{ij} have the same numerical values as δ^i_j above.

2.2.2 Spherical polar coordinate system

We introduce the spherical polar coordinates $(x^1, x^2, x^3) = (\vartheta, \lambda, r)$ as follows: ϑ is the colatitude (positive southwards), $0 \leqslant \vartheta \leqslant \pi$, λ is the longitude (positive eastwards) $(0 \leqslant \lambda < 2\pi)$ and $r \geqslant 0$ is the radial distance. Then the metric tensor reads

$$G_{ij} = \begin{bmatrix} r^2 & 0 & 0 \\ 0 & r^2 \sin^2 \vartheta & 0 \\ 0 & 0 & 1 \end{bmatrix}, \qquad G^{ij} = \begin{bmatrix} r^{-2} & 0 & 0 \\ 0 & r^{-2} \sin^{-2} \vartheta & 0 \\ 0 & 0 & 1 \end{bmatrix}. \tag{2.4}$$

The Christoffel symbols are

$$\left.\begin{aligned} \Gamma^1_{ij} &= \begin{bmatrix} 0 & 0 & r^{-1} \\ 0 & -\sin\vartheta\cos\vartheta & 0 \\ r^{-1} & 0 & 0 \end{bmatrix}, \qquad \Gamma^2_{ij} = \begin{bmatrix} 0 & \cot\vartheta & 0 \\ \cot\vartheta & 0 & r^{-1} \\ 0 & r^{-1} & 0 \end{bmatrix}, \\ \Gamma^3_{ij} &= \begin{bmatrix} -r & 0 & 0 \\ 0 & -r\sin^2\vartheta & 0 \\ 0 & 0 & 0 \end{bmatrix}. \end{aligned}\right\} \tag{2.5}$$

It is more common to use the spherical polar coordinates $(x^1, x^2, x^3) = (r, \vartheta, \lambda)$. Our choice of $(x^1, x^2, x^3) = (\vartheta, \lambda, r)$ is more suitable if we wish to describe interfaces in the form $x^3 = f(x^1, x^2)$.

2.2.3 Geographic spherical coordinate system

We introduce the geographic spherical coordinates $(x^1, x^2, x^3) = (\lambda, \vartheta, r)$ as follows: λ is the longitude (positive eastwards) $(0 \leqslant \lambda < 2\pi)$, ϑ is the latitude (positive northwards) $(-\frac{1}{2}\pi \leqslant \vartheta \leqslant \frac{1}{2}\pi)$ and $r \geqslant 0$ is the radial

distance. Then the metric tensor reads

$$G_{ij} = \begin{bmatrix} r^2\cos^2\vartheta & 0 & 0 \\ 0 & r^2 & 0 \\ 0 & 0 & 1 \end{bmatrix}, \qquad G^{ij} = \begin{bmatrix} r^{-2}\cos^{-2}\vartheta & 0 & 0 \\ 0 & r^{-2} & 0 \\ 0 & 0 & 1 \end{bmatrix}. \tag{2.6}$$

The Christoffel symbols are

$$\left.\begin{aligned} \Gamma^1_{ij} &= \begin{bmatrix} 0 & -\tan\vartheta & r^{-1} \\ -\tan\vartheta & 0 & 0 \\ r^{-1} & 0 & 0 \end{bmatrix}, \quad \Gamma^2_{ij} = \begin{bmatrix} \sin\vartheta\cos\vartheta & 0 & 0 \\ 0 & 0 & r^{-1} \\ 0 & r^{-1} & 0 \end{bmatrix}, \\ \Gamma^3_{ij} &= \begin{bmatrix} -r\cos^2\vartheta & 0 & 0 \\ 0 & -r & 0 \\ 0 & 0 & 0 \end{bmatrix}. \end{aligned}\right\} \tag{2.7}$$

2.2.4 Other coordinate systems

Instead of the above coordinate systems, any other system may be used. For instance, if we consider the ellipticity of the Earth then ellipsoidal coordinates may be used. It is usually straightforward to write the metric tensor for other coordinate systems.

3 MODEL OF THE MEDIUM

3.1 The model

The model M is defined inside a volume of space,

$$M: \quad x^i_{\min} \leqslant x^i \leqslant x^i_{\max} \quad (i = 1, 2, 3), \tag{3.1}$$

by functions specifying the distribution of the parameters of the medium. The coordinate surfaces $x^i = x^i_{\min}$ and $x^i = x^i_{\max}$ are *boundaries of the model.* The parameters of the medium are, for example, P- and S-wave velocities, v_P, v_S, density ρ, loss factors Q_P^{-1}, Q_S^{-1}, or some powers of these quantities. In this way, the velocity distribution may be specified by velocity values, by values of the square of the velocity, by values of slowness, by values of quadratic slowness, etc. Likewise, instead of loss factors, their reciprocal values Q_P and Q_S, called quality factors, may be considered. The parameters of the medium must be smooth functions of the coordinates inside the model, where "smooth" means that the parameters and their first and second partial derivatives must be

continuous. The smoothness of their distribution may be violated at a finite set of interfaces across which the parameters or their first or second partial derivatives may be discontinuous.

We consider models in which every such interface may be covered by a finite number of *smooth surfaces* $\Sigma: f(x^i) = 0$ with the following property: the functions $f(x^i)$ are defined and are smooth in the whole M i.e. $f(x^i)$ and their first and second derivatives are continuous everywhere in M. The surfaces may intersect each other. They may cross the whole model and intersect the boundaries of the model; they may also form closed surfaces (e.g. of ellipsoidal form) inside the model M. Each surface divides the whole model into two parts, the *positive part,* in which $f(x^i) > 0$, and the *negative part,* in which $f(x^i) < 0$. Accordingly, the side of the surface that faces the positive part of the model is called the *positive side of the surface* Σ, the other one being the *negative side of the surface* Σ. The smooth surfaces Σ may be indexed in ascending order by integers, starting from 1.

As in Gjøystdal *et al.* (1985), we construct the model from two types of blocks formed by smooth surfaces Σ: simple blocks (SB), which are the "building bricks" of our model and have no physical meaning, and complex blocks (CB), which represent the physical units of the model. We distinguish between *material blocks,* in which the density is always non-zero and positive, and *free-space blocks,* in which the density is identically zero.

A *simple block* (*SB*) is defined by two finite sets F^+ and F^- of surfaces $f(x^i) = 0$. A point x^i lies within the block if and only if

$$\left.\begin{aligned} f(x^i) > 0 \quad & \text{for any } f \in F^+ \\ f(x^i) < 0 \quad & \text{for any } f \in F^-. \end{aligned}\right\} \tag{3.2}$$

The simple block is an intersection of the positive parts of the model corresponding to the surfaces from F^+ and the negative parts of the model corresponding to F^- (see Gjøystdal *et al.*, 1985). An example is shown in Fig. 1 (see Section 3.4). Only parts of the surfaces Σ may be boundaries of a block—the remaining parts being only fictitious extensions of the boundary. Boundaries of some simple blocks may also be partially formed by parts of the boundaries of the model. Note that a simple block may be formed by several separated regions, not only by one connected region.

The division of the model into simple blocks is not unique. The SBs need not form a disjoint system, i.e. a point of the model may be situated in several SBs. SBs may be indexed in ascending order by positive integers, starting from 1. It is reasonable to index only the material

blocks, and leave the free-space blocks without indices. In this way, the blocks without indices may be immediately identified as free spaces without checking whether the density is zero or non-zero.

The simple block concept does not allow consideration of blocks in which the fictitious extensions of boundaries of the block intrude into the block (see Fig. 2 in Section 3.4). This means that one "physical" block of the model may be simulated by several simple blocks. In order to avoid this artificial division of the model, which would also complicate coding of waves (see Section 4), we introduce complex blocks.

A *complex block* (*CB*) is formed as a union of several simple blocks (it may, of course, also be formed of just one simple block). It may be defined by a table giving the indices of simple blocks that should be included in the complex block. While the SBs need not form a disjoint system, the CBs must form one. Any point of the model must be situated in just one CB. The boundaries of CBs, which may also be called *interfaces,* are formed by boundaries of SBs. The CBs may be indexed by positive indices, starting from 1. The system of indexing the blocks may be arbitrary, but some systems may render computations more effective. The material complex blocks must contain only material SBs. The complex block formed of free-space SBs is called the free-space complex block.

Note that in the following sections we shall introduce additional surfaces, which have the same properties and may be specified in the same way as the smooth surfaces Σ described above. However, they have a different meaning. The purpose of one set of these surfaces is to store all the quantities obtained by complete ray tracing; otherwise they are fully transparent, i.e. they have no effect on the ray tracing (see Section 5.5.2). The other set contains surfaces at which the complete ray tracing is to terminate (see Section 5.4, case (f)).

3.2 The data and routines specifying the model

The specification of data defined in Section 3.2.1 and routines defining the surfaces $f(x^i) = 0$ and the parameters of the medium (see Sections 3.2.2 and 3.2.3) fully determine the model.

3.2.1 Data specifying the model

(a) Indices NEXPV, NEXPQ specifying exponents of the power of velocities (NEXPV) and loss-factors (NEXPQ) in input data. For example, unit indices NEXPV and NEXPQ indicate that para-

meters of the medium are velocities and loss-factors, indices equal to -1 indicate reciprocal values of these quantities, i.e. slowness and quality factors.

(b) The boundaries of the model $x^1_{\min}$, $x^1_{\max}$, $x^2_{\min}$, $x^2_{\max}$, $x^3_{\min}$, $x^3_{\max}$.

(c) The number NSRFC of smooth surfaces Σ in the model. The surfaces are indexed sequentially by positive integers, from 1 to NSRFC.

(d) The number NSB of material simple blocks in the model. The blocks are indexed sequentially by positive integers ISB, from 1 to NSB. The free-space blocks are not indexed.

(e) For each simple block with index ISB, the indices of the surfaces forming the set F^+_{ISB} and the indices of the surfaces forming the set F^-_{ISB}. The indices of surfaces from F^+_{ISB} are stored with positive signs; the indices of surfaces from F^-_{ISB} are stored with negative signs. The indices may be specified in an arbitrary order.

(f) The number NCB of material complex blocks in the model. The blocks are indexed sequentially by positive integers ICB, from 1 to NCB. The free-space blocks are not indexed.

(g) For each complex block, the indices of simple blocks forming the complex block. The indices may be specified in an arbitrary order.

3.2.2 Specification of smooth surfaces

The functions $f(x^i)$ may be specified with the use of simple analytic expressions, interpolation or approximation of values given at discrete points, and so on. The coefficients of these functions may be prepared in the user-defined routine SRFC1, in which the input data concerning the surfaces $f(x^i) = 0$ may also be read in. The functional values as well as the first and second partial derivatives of the functions $f(x^i)$ at a specified point may be obtained by a user-defined routine called SRFC2 here.

3.2.3 Specification of the parameters of the medium

The distribution of the parameters of the medium in each complex block may be specified by simple analytic expressions, by interpolation or approximation of values given at discrete points, etc. The parameters may be either P- and S-wave velocities, density and loss-factors, or their powers. The distribution of any of these parameters may also be expressed in terms of the distribution of another parameter, for example, $v_S = 0.577 v_P$ or $\rho = 1.7 + 0.2 v_P$, where v_P, v_S and ρ are P and S velocities and density. The coefficients of these functions may be prepared in a user-defined routine called PARM1 here, in which the input data

concerning the distribution of individual parameters within each complex block may be read in. The functional values as well as the first and second partial derivatives of these functions may be obtained in a user-defined routine PARM2.

3.3 Auxiliary procedures

For complete ray tracing, some auxiliary procedures specifying the position of a point with respect to simple and complex blocks and smooth surfaces, or transforming the specified parameters of medium into velocities, density and loss factors, may be useful. The auxiliary procedures do not specify the model, they are only service procedures for complete ray tracing.

3.3.1 Determination of the index of a block

For the determination of the index of a simple and a complex block, in which a specified point (e.g. point source) is situated, a routine, called BLOCK here, may be used. This routine may also be used to determine the index of a block touching a specified block at a point situated on the boundary of the specified block (the situation that may arise when a ray impinges on a boundary of a block). Another function of the routine may be to determine the index of a surface bounding a block and separating the block from the given point (surface $f(x^i) = 0$ separates sets A and B if $f(x^i)f(y^i) < 0$ for any $x^i \in A$, $y^i \in B$).

3.3.2 Transformation of the parameters of the medium

The routine transforming the values of the parameters of the medium into the velocity and loss factor of the corresponding type of wave is called VELOC here.

3.4 Examples

We present several examples of how to build models for complete ray tracing. We present cross-sections of 3D models specified in Cartesian coordinates. Of course, they may also be interpreted as 2D models. Individual figures always contain a picture of the model and a picture (or pictures) of its representation in terms of simple blocks. The parts of the model below smooth surfaces are considered as positive, those above

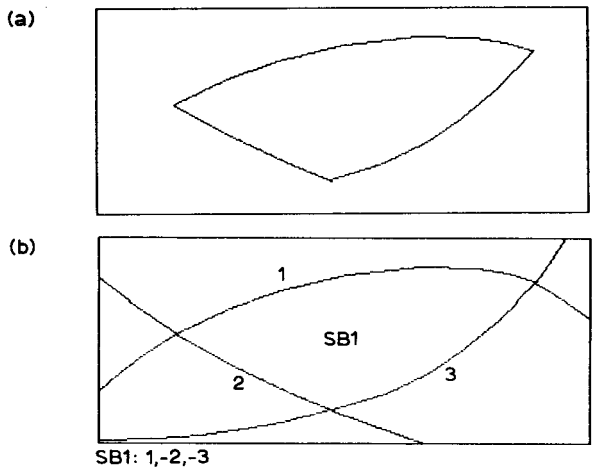

Fig. 1 (a) Simple block. (b) Its representation by three surfaces indexed 1, 2, 3.

them as negative parts of the model. In the case of a closed surface the positive part of the model is situated outside the closed surface. The tables attached to the figures specify the indices of surfaces belonging to the sets F^{+}_{ISB} (positive numbers) and F^{-}_{ISB} (absolute values of negative numbers) for each simple block ISB.

To better understand the individual figures of the models shown later in this section, let us first show a schematic picture of a simple block (see Fig. 1). Similarly, Fig. 2 shows that one physical (complex) block may be simulated by several simple blocks in various ways.

Example 1: Layered structure

Figure 3(a) shows a model of a simple layered structure. The layers are separated by non-intersecting smooth interfaces. The representation of such a structure in terms of simple blocks (see Fig. 3b) is very simple. Each interface is represented by one smooth surface Σ, each layer by one simple block. Complex blocks are in this case identical with the simple blocks.

Example 2: Isolated body A

Figure 4(a) shows a layered structure containing an isolated body. The representation of the model in terms of simple blocks for two different systems of indexing surfaces and SBs is shown in Figs 4(b,c). It is again

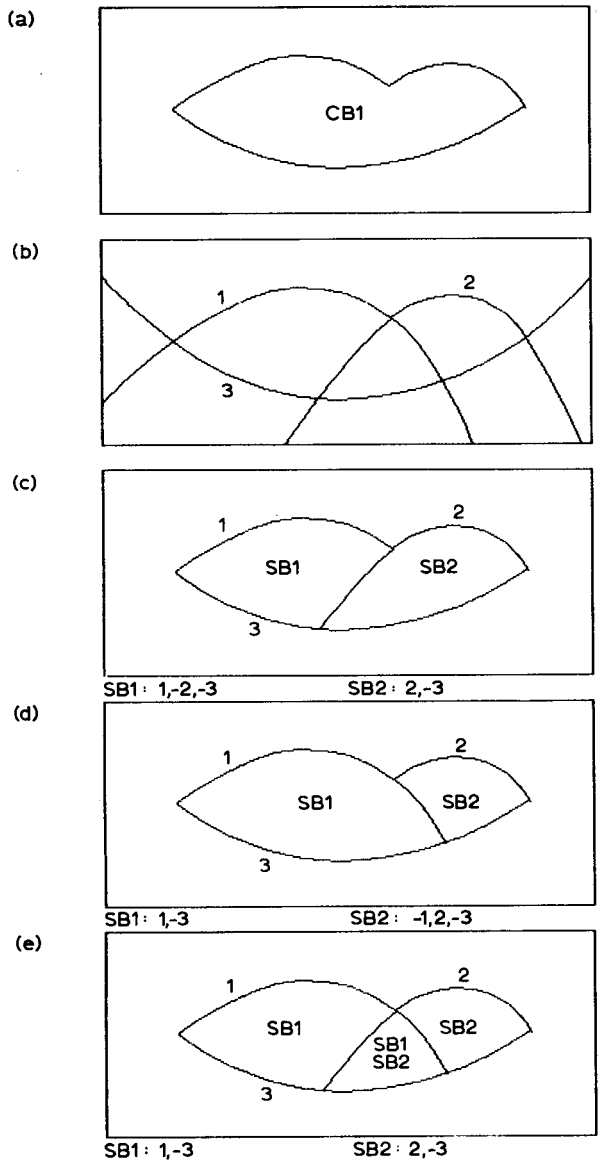

Fig. 2 (a) Complex block. (b) Three surfaces 1, 2, 3 covering the boundary of (a). (c, d, e) Construction of the complex block (a) using two simple blocks in several ways.

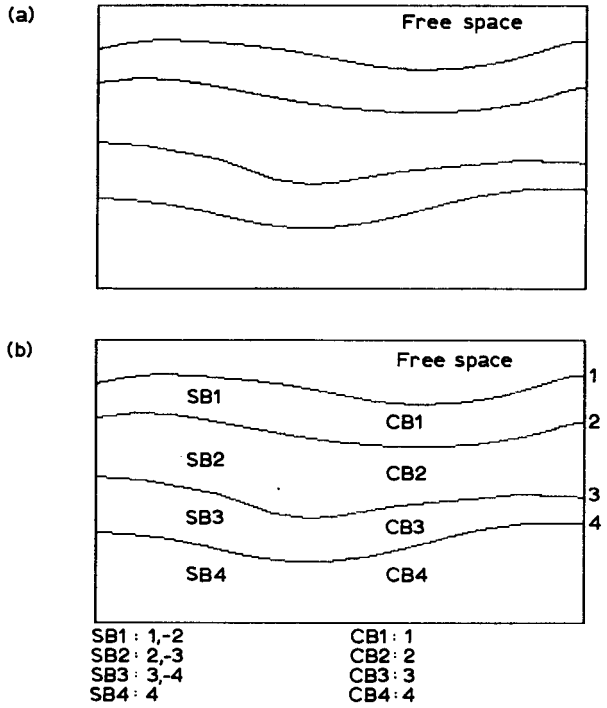

Fig. 3 (a) Model of a simple layered structure. (b) Its computer representation.

very simple. Each interface is represented by one smooth surface, surfaces 2 in Fig. 4(b) and 1 in Fig. 4(c) being closed surfaces. An isolated body represents one simple block, the remaining part of the layer another one. Complex blocks are again identical with simple blocks. In both pictures, (b) and (c), complex blocks are indexed from the top to the bottom.

Example 3: Isolated body B

Figure 5(a) shows a model of a layered structure containing an isolated body with edges. Possible representations of the model in terms of simple blocks are shown in Figs 5(b,c). This example shows that: (i) the division of models into simple blocks may be non-unique; (ii) although the region represented by simple blocks 1 and 3 is one physical unit (see Fig. 5a), it cannot be represented by a single simple block (the region contains points that are situated both in positive and negative parts of the model

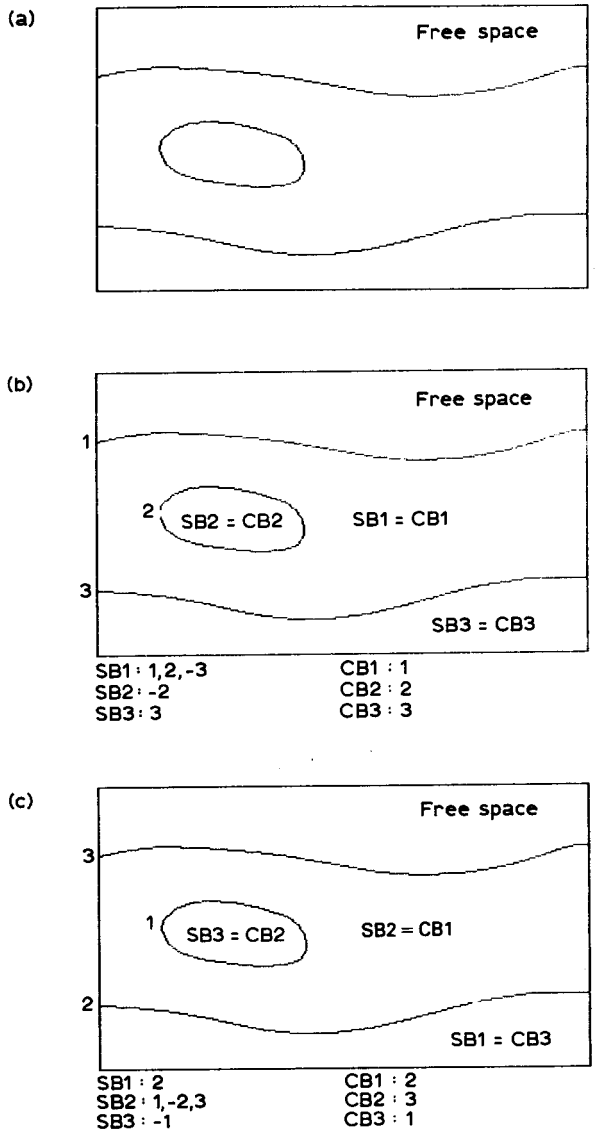

Fig. 4 (a) Model of a smooth isolated body. (b, c) Its two computer representations.

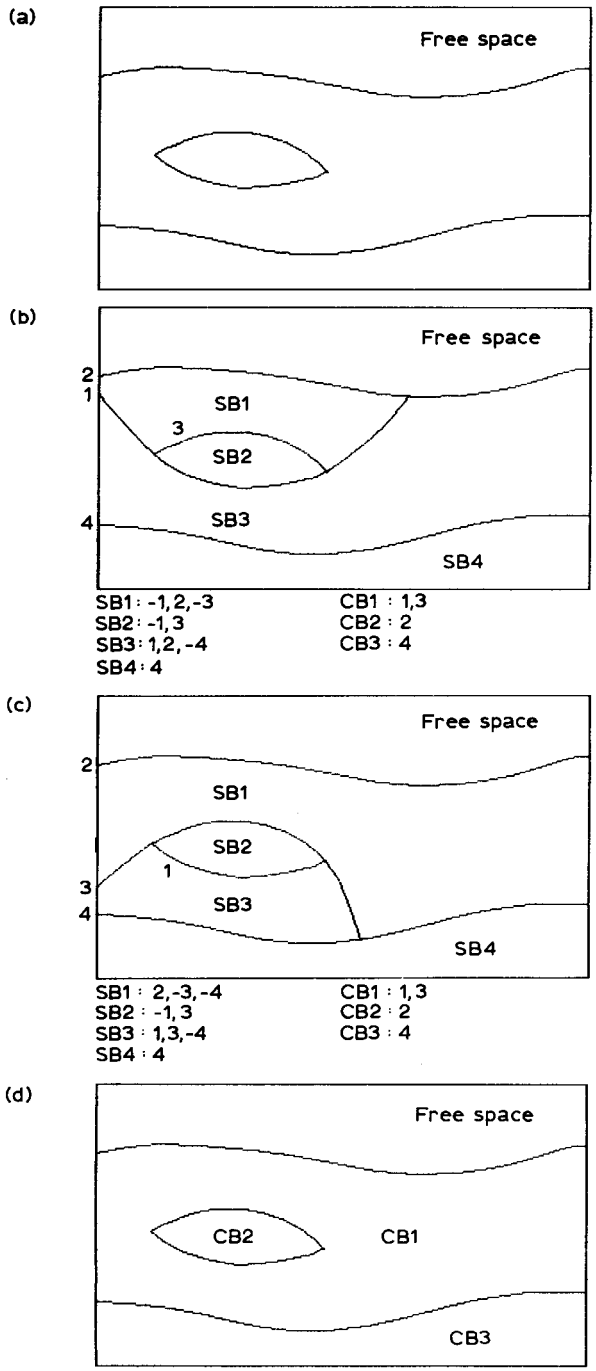

Fig. 5 (a) Model of an isolated body with edges. (b, c) Its two computer representations in terms of simple blocks. The complex blocks in the two representations are equivalent—see (d).

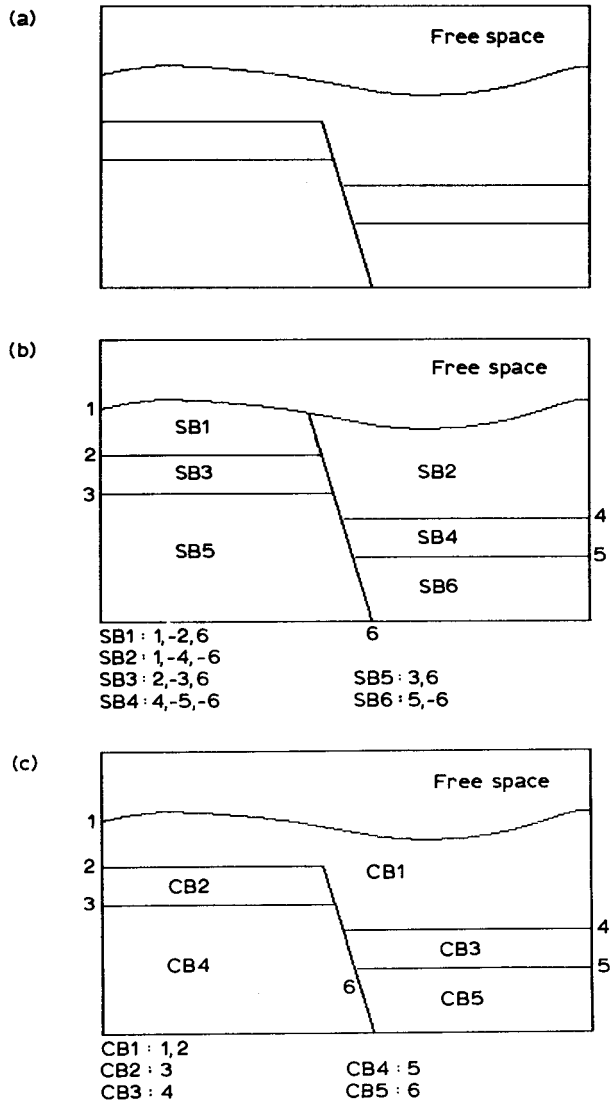

Fig. 6 (a) Model of a fracture structure with a sedimentary cover. (b) Its computer representation in terms of simple blocks. (c) Its computer representation in terms of complex blocks.

with respect to the smooth surface 1 or 3—see also Fig. 2). The simple blocks 1 and 3, however, may be united to form a complex block of the same physical properties (see Fig. 5d). Complex blocks 2 and 3 are identical with the simple blocks.

Example 4: Fracture structure

Figure 6(a) shows a model of a simple fracture structure with a sedimentary cover. Its representation in terms of simple blocks is shown in Fig. 6(b). Simple blocks 1 and 2 may be united to form a complex block, the other complex blocks are identical with simple blocks.

4 CODES FOR ELEMENTARY WAVES

We consider ordinary seismic body waves, such as refracted, primarily or multiply reflected, possibly converted waves. In general, incidence of a wave at an interface (boundary of a complex block) produces four waves, reflected P and S, and transmitted P and S waves. When performing complete ray tracing, we must know a priori which of the four generated waves to follow. This decision must be made at each interface. The alphanumeric string specifying the behaviour of a ray from its initial point to its endpoint is a *code.*

The term *elementary wave* does not have unique meaning in the literature. Here we apply the term to that part of the wavefield that is described by one specific code. Since there may be various types of codes, there is also a variety of divisions of the wavefield into the elementary waves.

We introduce the term *element of a ray,* which has an important meaning in the construction of codes. By an element of a ray, we denote that part of the ray that is situated in one complex block between two successive points of reflection/transmission, or between the initial point or endpoint of the ray and the closest point of reflection/transmission or between the initial point and the endpoint of the ray, if the ray is entirely situated in one complex block.

There are many possible types of codes of elementary waves. Usually they are given by a finite sequence of non-zero integers. For the transformation of the code into instructions specifying the behaviour of the considered elementary wave at the initial points of rays and at all points of incidence at interfaces (boundaries of complex blocks), a routine, called CODE here, should be prepared.

5 COMPLETE RAY TRACING

5.1 Theory

Complete ray tracing consists of: (a) ray tracing and computation of the travel time along the ray; (b) determination of the polarization vectors along the ray; (c) dynamic ray tracing (i.e. computation of the ray propagator matrix); (d) determination of the vectorial complex-valued reduced amplitudes.

5.1.1 *Ray tracing and travel-time computation*

Ray tracing consists in the computation of a ray, i.e. in a step-by-step evaluation of coordinates of points along the ray. The ray is parametrized by an independent variable

$$\sigma = \sigma_0 + \int_{\tau_0}^{\tau} v^{\mathrm{NEXPS}}\,\mathrm{d}\tau = \sigma_0 + \int_{s_0}^{s} v^{\mathrm{NEXPS}-1}\,\mathrm{d}s, \tag{5.1}$$

where τ is the travel time, s is the arclength along the ray and v is the velocity of the corresponding type of wave. The integer exponent NEXPS may be specified by a user, NEXPS = 0, $\pm 1, \pm 2, \ldots$. We consider the ray-tracing system in the form of a system of six first-order ordinary differential equations:

$$\left.\begin{aligned} \frac{\mathrm{d}x^i}{\mathrm{d}\sigma} &= v^{2-\mathrm{NEXPS}} G^{ij} p_j, \\ \frac{\mathrm{d}p_i}{\mathrm{d}\sigma} &= v^{2-\mathrm{NEXPS}}\left(- v^{-3}\frac{\partial v}{\partial x^i} + \Gamma_{ij}^k G^{jl} p_k p_l \right). \end{aligned}\right\} \tag{5.2}$$

Here x^i are the coordinates of a point along the ray, p_i are the covariant components of the slowness vector at the point x^i, and $p_i = \partial\tau/\partial x^i$. For the metric tensor G^{ij} and the Christoffel symbols Γ_{ij}^k see Section 2. At an interface, the ray is transformed using the Snell law.

The equation

$$\tau = \tau_0 + \int_{\sigma_0}^{\sigma} v^{-\mathrm{NEXPS}}\,\mathrm{d}\sigma \tag{5.3}$$

for the real-valued travel time follows from (5.1). The imaginary part of the complex-valued travel time is defined as

$$\tau^{\mathrm{IM}} = \tfrac{1}{2}t^* = \int_{\tau_0}^{\tau} (2Q)^{-1}\,\mathrm{d}\tau = \int_{\sigma_0}^{\sigma} (2Q)^{-1} v^{-\mathrm{NEXPS}}\,\mathrm{d}\sigma, \tag{5.4}$$

where Q is the relevant quality factor.

5.1.2 Polarization vectors

Let us consider an arbitrarily selected ray and denote it by Ω. The determination of the polarization vectors along the ray Ω plays an important role in complete ray tracing for several reasons. The polarization vectors must be known if we wish to determine the orientation of the displacement vector of the wave propagating along Ω, especially in the case of S waves. Moreover, the polarization vectors form the vector basis of the *ray-centred coordinate system* connected with Ω. The ray-centred coordinate system is very useful in many applications, especially in dynamic ray tracing (see Section 5.1.3).

The orthogonal ray-centred coordinate system was introduced into seismology by Popov and Pšenčík (1978a,b). We shall denote the ray-centred coordinates by $(q^1, q^2, q^3 = s)$, where s is the arclength along the ray Ω, and q^K are the Cartesian coordinates in the plane tangent to the wavefront at point $s = q^3$ on Ω, with the origin on the ray Ω. The vector basis of the ray-centred coordinate system consists of three unit vectors $\boldsymbol{e}_1$, $\boldsymbol{e}_2$, $\boldsymbol{e}_3$ (polarization vectors), where $\boldsymbol{e}_3$ is tangent to the ray Ω, and $\boldsymbol{e}_1$ and $\boldsymbol{e}_2$ are perpendicular to Ω. They are introduced in such a way as to render the ray-centred coordinate system orthogonal. The equation

$$\frac{\mathrm{d}H_{ij}}{\mathrm{d}\sigma} = v^{1-\mathrm{NEXPS}}\left[\frac{\partial v}{\partial x^k} G^{kl} H_{lj} p_i - p_k G^{kl} H_{lj} \frac{\partial v}{\partial x^i} + v\Gamma^m_{ik} G^{kl} p_l H_{mj}\right] \tag{5.5}$$

holds for the covariant components H_{ij} of the ray-centred basis vector $\boldsymbol{e}_j$, $(\boldsymbol{e}_j)_i = H_{ij}$. This equation simplifies to

$$\frac{\mathrm{d}H_{iJ}}{\mathrm{d}\sigma} = v^{1-\mathrm{NEXPS}}\left[\frac{\partial v}{\partial x^k} G^{kl} H_{lJ} p_i + v\Gamma^m_{ik} G^{kl} p_l H_{mJ}\right] \tag{5.6}$$

for vectors $\boldsymbol{e}_J$ perpendicular to the ray Ω. For the unit vector $\boldsymbol{e}_3$ tangent to the ray Ω ($j = 3$ in (5.5)),

$$H_{i3} = v p_i = G_{ij} \frac{\mathrm{d}x^j}{\mathrm{d}s}, \tag{5.7}$$

and (5.5) is equivalent to the second equation of the ray-tracing system (5.2). It is sufficient to compute only the covariant components H_{i1} ($i = 1, 2, 3$) of the vector $\boldsymbol{e}_1$, because $\boldsymbol{e}_3$ is determined by (5.7) when the ray tracing (5.2) is performed, and because $\boldsymbol{e}_2$ is always perpendicular to both $\boldsymbol{e}_1$ and $\boldsymbol{e}_3$:

$$H_{i2} = \varepsilon_{ijk} G^{jm} H_{m3} G^{kn} H_{n1} [\det (G^{rs})]^{-1/2}. \tag{5.8}$$

Here $\varepsilon_{123} = \varepsilon_{231} = \varepsilon_{312} = 1$, $\varepsilon_{132} = \varepsilon_{321} = \varepsilon_{213} = -1$, $\varepsilon_{ijk} = 0$ for all other combinations of ijk. At an interface, the ray-centred coordinate system is

rotated around the vector perpendicular to the plane of incidence in such a way that, after the rotation, the vector $\boldsymbol{e}_3$ coincides with the tangent to the ray of the generated wave under consideration.

5.1.3 Dynamic ray tracing. Ray propagator matrix

Dynamic ray tracing consists in the solution of the system of four first-order linear differential equations along the ray Ω, for the components of a 4×1 column matrix $\boldsymbol{W}$,

$$\frac{\mathrm{d}\boldsymbol{W}}{\mathrm{d}\sigma} = v^{2-\mathrm{NEXPS}}\boldsymbol{S}\boldsymbol{W}, \tag{5.9}$$

where

$$\boldsymbol{S} = \begin{bmatrix} \boldsymbol{0} & \boldsymbol{I} \\ -v^{-3}\boldsymbol{V} & \boldsymbol{0} \end{bmatrix},$$

$\boldsymbol{0}$ and $\boldsymbol{I}$ being zero and identity 2×2 matrices, and $\boldsymbol{V}$ a 2×2 matrix with components

$$V_{IJ} = \left(\frac{\partial^2 v}{\partial x^k \, \partial x^l} - \Gamma^m_{kl}\frac{\partial v}{\partial x^m}\right) G^{kr} G^{ls} H_{rI} H_{sJ}. \tag{5.10}$$

The first two components of $\boldsymbol{W}$ are ray-centred coordinates (q^1, q^2) of a paraxial ray (up to first order in Taylor expansion), and the other two components of $\boldsymbol{W}$ are the corresponding ray-centred components of the slowness vector of the paraxial ray.

The dynamic ray-tracing system (5.9) has four linearly independent solutions. We denote by $\boldsymbol{\Pi}(\sigma, \sigma_0)$ the fundamental 4×4 matrix of linearly independent solutions of (5.9) with the initial condition

$$\boldsymbol{\Pi}(\sigma_0, \sigma_0) = \boldsymbol{I}$$

at the initial point $\sigma = \sigma_0$ of the ray. Here $\boldsymbol{I}$ is the 4×4 identity matrix. The fundamental matrix $\boldsymbol{\Pi}(\sigma, \sigma_0)$ is also called the ray propagator matrix, or the propagator matrix of the dynamic ray-tracing system. It satisfies the following relation along the ray:

$$\boldsymbol{\Pi}^{\mathrm{T}}\boldsymbol{\Sigma}\boldsymbol{\Pi} = \boldsymbol{\Sigma}, \quad \text{with } \boldsymbol{\Sigma} = \begin{bmatrix} 0 & 0 & 1 & 0 \\ 0 & 0 & 0 & 1 \\ -1 & 0 & 0 & 0 \\ 0 & -1 & 0 & 0 \end{bmatrix}. \tag{5.11}$$

This is the so-called symplectic property of $\boldsymbol{\Pi}$. Any solution $\boldsymbol{W}(\sigma)$ of the

dynamic ray-tracing system (5.9) can be expressed in the form

$$\boldsymbol{W}(\sigma) = \boldsymbol{\Pi}(\sigma, \sigma_0)\boldsymbol{W}(\sigma_0). \tag{5.12}$$

Solutions of the dynamic ray-tracing system (5.9) have found many important applications in seismology. Let us assume that the computed ray belongs to a two-parameter system of rays, parametrized by ray parameters γ^1, γ^2. Then, the dynamic ray-tracing system can be used to determine the 2×2 matrices $\boldsymbol{Q}^{\mathrm{R}}$ and $\boldsymbol{P}^{\mathrm{R}}$ along the ray, with elements

$$\left.\begin{aligned} Q^{\mathrm{R}}_{IJ} &= \left[\frac{\partial q^I}{\partial \gamma^J}\right]_{q^1=q^2=0}, \\ P^{\mathrm{R}}_{IJ} &= \left[\frac{\partial^2 \tau}{\partial q^I \partial \gamma^J}\right]_{q^1=q^2=0} = \left[\frac{\partial p_I^{(q)}}{\partial \gamma^J}\right]_{q^1=q^2=0}. \end{aligned}\right\} \tag{5.13}$$

Here q^I are the ray-centred coordinates of a paraxial ray specified by ray parameters γ^1, γ^2; $p_I^{(q)}$ are the relevant ray-centred components of the slowness vector of the paraxial ray, $p_I^{(q)} = \partial\tau/\partial q^I$. The matrix $\boldsymbol{Q}^{\mathrm{R}}$ is also called the matrix of geometrical spreading, $|\det \boldsymbol{Q}^{\mathrm{R}}|$ being the geometrical spreading. It measures the expansion and contraction of the ray tube. The geometrical spreading is dependent on the parametrization of the rays.

We introduce the ray coordinates $(\gamma^1, \gamma^2, \gamma^3)$, where γ^1 and γ^2 are the ray parameters and γ^3 is a parameter along the ray (e.g. the arclength s). Then the matrix $\boldsymbol{Q}^{\mathrm{R}}$ may be also interpreted as the transformation matrix from ray coordinates (γ^1, γ^2) to the ray-centred coordinates (q^1, q^2) along the ray Ω. Similarly, the matrix $\boldsymbol{P}^{\mathrm{R}}$ represents the transformation matrix from ray coordinates (γ^1, γ^2) to the "phase-space" coordinates $p_1^{(q)}$, $p_2^{(q)}$. The 4×2 matrix $\boldsymbol{X}^{\mathrm{R}}$, defined as

$$\boldsymbol{X}^{\mathrm{R}} = \begin{bmatrix} \boldsymbol{Q}^{\mathrm{R}} \\ \boldsymbol{P}^{\mathrm{R}} \end{bmatrix}, \tag{5.14}$$

satisfies the dynamic ray-tracing system

$$\frac{\mathrm{d}\boldsymbol{X}^{\mathrm{R}}}{\mathrm{d}\sigma} = v^{2-\mathrm{NEXPS}}\boldsymbol{S}\boldsymbol{X}^{\mathrm{R}} \tag{5.15}$$

along the ray Ω. The solution of (5.15) may be expressed in the form

$$\boldsymbol{X}^{\mathrm{R}}(\sigma) = \boldsymbol{\Pi}(\sigma, \sigma_0)\boldsymbol{X}^{\mathrm{R}}(\sigma_0). \tag{5.16}$$

If $\boldsymbol{Q}^{\mathrm{R}}$ and $\boldsymbol{P}^{\mathrm{R}}$ are known then we can also determine the 2×2 matrix of the second derivatives of the travel-time field $\boldsymbol{M}^{\mathrm{R}}(\sigma)$, with elements

$$M^{\mathrm{R}}_{IJ} = \left[\frac{\partial^2 \tau}{\partial q^I \partial q^J}\right]_{q^1=q^2=0}. \tag{5.17}$$

$\boldsymbol{Q}^{\mathrm{R}}$, $\boldsymbol{P}^{\mathrm{R}}$ and $\boldsymbol{M}^{\mathrm{R}}$ are related by

$$\boldsymbol{M}^{\mathrm{R}} = \boldsymbol{P}^{\mathrm{R}}(\boldsymbol{Q}^{\mathrm{R}})^{-1}. \tag{5.18}$$

The transformation of solutions of the dynamic ray-tracing system across interfaces is determined by Snell's law for paraxial rays.

5.1.4 *Vectorial reduced amplitudes*

Vectorial reduced amplitudes

$$A_i = A_i^{\mathrm{R}}(\rho v\, |\det \boldsymbol{Q}^{\mathrm{R}}|)^{1/2} \tag{5.19}$$

are the complex-valued vectorial displacement ray amplitudes A_i^{R} (including a phase shift due to caustics) expressed in the ray-centred coordinate system, multiplied by the square root of the impedance (product of density ρ and velocity v) and of the geometrical spreading $|\det \boldsymbol{Q}^{\mathrm{R}}|$. The vectorial reduced amplitudes A_i are assumed to be unity at the initial point of a ray. If the initial point is situated at the free surface or at any internal interface then the conversion coefficients may be included in A_i.

We define the 3×3 matrix A_{ij} composed of the vectorial reduced amplitude A_{i1} corresponding to the S wave polarized in the direction of the vector $\boldsymbol{e}_1$ at the initial point of the ray, of the vectorial reduced amplitude A_{i2} corresponding to the S wave polarized in the direction of $\boldsymbol{e}_2$ at the initial point, and of the vectorial reduced amplitude A_{i3} corresponding to the P wave at the initial point. The components of the vectorial reduced amplitudes A_{ij} are expressed in the ray-centred coordinate system. They are constant along the elements of a ray inside individual blocks, except at caustics, where they must be multiplied by $-\mathrm{i}$ or -1, according to the type of caustic. At interfaces, the vectorial reduced amplitudes are transformed by means of reduced reflection/transmission (R/T) coefficients

$$R^{\mathrm{E}} = R\left[\frac{\tilde{\rho}\tilde{v}\,|\cos\tilde{\alpha}|}{\rho v\,|\cos\alpha|}\right]^{1/2}, \tag{5.20}$$

where R are plane-wave displacement reflection/transmission coefficients. Here the quantities with a tilde correspond to the relevant R/T wave, those without tilde to the incident wave; in both cases at the point of incidence. α and $\tilde{\alpha}$ are the angles of incidence and of R/T respectively.

5.2 Quantities computed along a ray

5.2.1 Basic quantities computed along a ray

Complete ray tracing is performed to compute the following basic quantities at selected points along a ray:

$\mathrm{Y}(1) = \tau$ travel time;

$\mathrm{Y}(2) = \tau^{\mathrm{IM}} = \frac{1}{2}t^*$ imaginary part of the complex-valued travel time;

$\left.\begin{aligned}\mathrm{Y}(3) &= x^1\\ \mathrm{Y}(4) &= x^2\\ \mathrm{Y}(5) &= x^3\end{aligned}\right\}$ coordinates of points along the ray;

$\left.\begin{aligned}\mathrm{Y}(6) &= p_1\\ \mathrm{Y}(7) &= p_2\\ \mathrm{Y}(8) &= p_3\end{aligned}\right\}$ covariant components of the slowness vector;

$\left.\begin{aligned}\mathrm{Y}(9) &= H_{11}\\ \mathrm{Y}(10) &= H_{21}\\ \mathrm{Y}(11) &= H_{31}\end{aligned}\right\}$ covariant components of the polarization vector $\boldsymbol{e}_1$, see (5.6) for $J = 1$;

$$\begin{bmatrix} \mathrm{Y}(12) & \mathrm{Y}(16) & \mathrm{Y}(20) & \mathrm{Y}(24)\\ \mathrm{Y}(13) & \mathrm{Y}(17) & \mathrm{Y}(21) & \mathrm{Y}(25)\\ \mathrm{Y}(14) & \mathrm{Y}(18) & \mathrm{Y}(22) & \mathrm{Y}(26)\\ \mathrm{Y}(15) & \mathrm{Y}(19) & \mathrm{Y}(23) & \mathrm{Y}(27)\end{bmatrix} = \begin{bmatrix} \Pi_{11} & \Pi_{12} & \Pi_{13} & \Pi_{14}\\ \Pi_{21} & \Pi_{22} & \Pi_{23} & \Pi_{24}\\ \Pi_{31} & \Pi_{32} & \Pi_{33} & \Pi_{34}\\ \Pi_{41} & \Pi_{42} & \Pi_{43} & \Pi_{44}\end{bmatrix},$$

the matrix of fundamental solutions of the dynamic ray tracing system (5.9) (ray propagator matrix);

$\mathrm{Y}(28), \ldots, \mathrm{Y}(\mathrm{NY})$, where $\mathrm{NY} = 27 + \mathrm{NAMPL}$.

There are NAMPL real quantities representing complex-valued vectorial reduced amplitudes. The vectorial reduced amplitudes are specified in the ray-centred coordinate system. Here NAMPL may be either 2, 4 or 8, in the following alternative cases:

(a_1) Case of a P wave at the initial point of the ray, and of a P wave at the point under consideration on the ray. Then NAMPL = 2, and

$\mathrm{Y}(28) = \mathrm{Re}\, A_{33}$, $\mathrm{Y}(29) = \mathrm{Im}\, A_{33}$.

(a_2) Case of a P wave at the initial point of the ray, and of an S wave at the point under consideration on the ray. Then NAMPL = 4, and

$Y(28) = \mathrm{Re}\, A_{13}$, $Y(29) = \mathrm{Im}\, A_{13}$,

$Y(30) = \mathrm{Re}\, A_{23}$, $Y(31) = \mathrm{Im}\, A_{23}$.

(b_1) Case of an S wave at the initial point of the ray, and of a P wave at the point under consideration on the ray. Then NAMPL = 4, and

$Y(28) = \mathrm{Re}\, A_{31}$, $Y(29) = \mathrm{Im}\, A_{31}$,

$Y(30) = \mathrm{Re}\, A_{32}$, $Y(31) = \mathrm{Im}\, A_{32}$.

(b_2) Case of an S wave at the initial point of the ray, and of an S wave at the point under consideration on the ray. Then NAMPL = 8, and

$Y(28) = \mathrm{Re}\, A_{11}$, $Y(29) = \mathrm{Im}\, A_{11}$,

$Y(30) = \mathrm{Re}\, A_{21}$, $Y(31) = \mathrm{Im}\, A_{21}$,

$Y(32) = \mathrm{Re}\, A_{12}$, $Y(33) = \mathrm{Im}\, A_{12}$,

$Y(34) = \mathrm{Re}\, A_{22}$, $Y(35) = \mathrm{Im}\, A_{22}$.

5.2.2 *Auxiliary quantities computed along a ray*

Knowledge of the basic quantities, described above, at a point of the ray Ω is not sufficient for continuation of complete ray tracing from the point. In this section we introduce some quantities that are necessary or useful for complete ray tracing, together with some quantities containing some information about ray tracing.

$YY(1) = \sigma$	independent variable along the ray.
YY(2) = UEBRAY	upper error bound for ray tracing, which is equal to the input value UEB at the initial point of the ray (see Section 5.6j). It is always doubled when the numerical integration requires more than NHLF bisections of the initial step STEP (see Section 5.6g). UEBRAY > UEB at the endpoint of the ray indicates a decreased accuracy of computation.

YY(3) = ERRPP YY(4) = ERRPH YY(5) = ERRHH	deviations (in absolute values) of the two computed basis vectors of the ray-centred coordinate system from the conditions of orthonormality (see Sections 5.8.2d and 5.8.3i), accumulated along the ray. Any of them may be compared with the corresponding specified limit UEBPP, UEBPH or UEBHH (see Section 5.6k) at the endpoint of the ray.
IY(1) = NY = 27 + NAMPL	number of basic quantities describing the point of a ray (see Section 5.2.1).
IY(2) = KODIND	position in the code corresponding to the considered element of a ray; its value is determined by subroutine CODE (see Section 4).
IY(3) = ICB0	index of the complex block from which the ray entered the complex block in which the computed element of the ray is situated; IY(3) = 0 before leaving the complex block in which the initial point of the ray is situated.
IY(4) = ISB1	index of the simple block containing the computed element of the ray.
IY(5) = ICB1	index of the complex block containing the computed element of the ray, supplemented by sign + for a P wave and sign − for an S wave.
IY(6) = ISRF	index of the surface at which the endpoint of the computed element of the ray is situated; undefined inside the complex block, defined only at the endpoint of the element of the ray.
IY(7) = ISB2	index of the simple block touching the complex block ICB1 from the other

	side of the surface ISRF at the endpoint of the computed element of the ray; ISB2 = 0 for a free space on the other side of ISRF; undefined inside the complex block, defined only at the endpoint of the element of the ray.
IY(8) = ICB2	index of the complex block touching the complex block ICB1 from the other side of the surface ISRF at the endpoint of the computed element of the ray; ICB2 = 0 for a free space on the other side of ISRF; undefined inside the complex block, defined only at the endpoint of the element of the ray.
IY(9) = IFCT	number of invocations of subroutine FCT evaluating the right-hand sides of the ordinary differential equations along the computed part of the ray.
IY(10) = IOUTP	number of successful steps of the numerical integration along the ray.
IY(11) = ITRANS	number of transformations at an interface.
IY(12) = KMAH	number of caustic points along the ray (the index of the ray trajectory).

5.2.3 *Quantities for the identification of caustics*

Computation of the reduced vectorial amplitudes requires knowledge of the position of caustics on the computed ray. The position of a caustic is not a property of a single ray, but a property of the rayfield. It depends on the mutual position of paraxial rays with respect to the computed ray. The mutual position can be determined if the 2×2 matrix

$$\boldsymbol{M}^{\mathrm{INIT}} = \boldsymbol{M}^{\mathrm{R}}(\sigma_0)$$

of the second derivatives of the travel-time field at the initial point $\sigma = \sigma_0$ of the computed ray is known. The matrix $\boldsymbol{M}^{\mathrm{INIT}}$ may be specified in terms of the matrices $\boldsymbol{Q}^{\mathrm{INIT}} = \boldsymbol{Q}^{\mathrm{R}}(\sigma_0)$ and $\boldsymbol{P}^{\mathrm{INIT}} = \boldsymbol{P}^{\mathrm{R}}(\sigma_0)$ (see Section 5.1.3) as

$$\boldsymbol{M}^{\mathrm{INIT}} = \boldsymbol{P}^{\mathrm{INIT}}(\boldsymbol{Q}^{\mathrm{INIT}})^{-1}.$$

5.3 Auxiliary surfaces

In addition to surfaces $1, \ldots,$ NSRFC covering structural interfaces and described in Section 3, some other (auxiliary) surfaces may be useful when we perform complete ray tracing. The surfaces may be used for the limitation of a computational volume for complete ray tracing (see Section 5.4) or for storing the computed quantities (see Section 5.5).

Note that the computational volume may be introduced as a subvolume of the model M under consideration. The actual computations are then performed only in the computational volume, not in the whole of M, and are terminated at the boundaries of the computational volume. This considerably increases the efficiency of computations performed in various regions of the model M.

The auxiliary surfaces are indexed by integers from NSRFC + 1 to NSRFC + NSRFCA, where NSRFCA is the number of auxiliary surfaces. The auxiliary surfaces may be described in the same way as the surfaces covering structural interfaces, the same routine SRFC1 may be used for reading input data and for the preparation of the necessary coefficients, and the same routine SRFC2 may be used for their evaluation.

The auxiliary surfaces are specified by their number NSRFCA, by the input data (read in by the subroutine SRFC1) and by the routine SRFC2.

5.4 Termination of tracing a ray

Computation of the ray Ω is terminated in the following cases:

(a) The computed ray satisfies the whole code, i.e. the last computed element of the ray corresponds to the last element in the code.

(b) At the point of incidence at an interface the ray cannot continue to satisfy the code. For example (i) the point of incidence may be situated at a different surface than that specified by the code; (ii) the next element of the ray may be required by the code to be situated in a block that does not touch the point of incidence (for

example, the code may require the transmission into a block that is not in contact with the block containing an incident ray at the point of incidence); (iii) transmission may be required by the code at a free surface; (iv) the ray of the required reflected or transmitted wave may not be real-valued (e.g. overcritical transmission); or (v) an S wave in a liquid block may be required by the code.

(c) Reflection or type conversion at a fictitious part of the interface is required by the code. The amplitudes of reflected or converted waves are zero in this case. In principle, each zero reflection/transmission coefficient could be a reason for the termination of the computation of the ray.

(d) The travel time Y(1) is greater than a specified time limit.

(e) The ray intersects any of the six coordinate planes ($x^i = x^i_{\mathrm{MIN}}$, $x^i = x^i_{\mathrm{MAX}}$) limiting the computational volume for complete ray tracing. The computational volume should not exceed the volume M in which the model is defined (see Section 3.1). Note that in addition to the six coordinate planes, auxiliary surfaces or model surfaces may also be used to limit the computational volume; see (f).

(f) The ray intersects any surface of the given set F_{END} of surfaces limiting the computational volume for complete ray tracing. The surfaces may be either surfaces that cover structural interfaces (see Section 3) or the auxiliary surfaces introduced in Section 5.3. The set F_{END} of surfaces is determined if the indices of the surfaces from F_{END} are specified and if the subroutine SRFC2 is activated.

5.5 Storage of computed quantities

The quantities computed along the rays and described in Section 5.2 may be stored in some files.

5.5.1 Storage of quantities along a ray

The quantities are stored along the whole computed ray with constant step STORE of the independent variable. The quantities at the points of intersection of the ray with interfaces are also stored. They may be, for instance, of use in plotting rays.

5.5.2 Storage of quantities at specified surfaces

The quantities are stored at the points of intersection of a ray with any surface from a given set F_{STORE}. The surfaces may be as follows.

(a) Surfaces $1, \ldots,$ NSRFC covering structural interfaces. The quantities are only stored along those parts of the surfaces that form the boundaries of complex blocks. Since the quantities are discontinuous across interfaces, we must specify, for each surface, its positive or negative side on which the quantities are to be stored. The sign denoting the positive or negative side may be included in the index of the surface.

(b) Auxiliary surfaces NSRFC + $1, \ldots,$ NSRFC + NSRFCA. The quantities are stored along the whole of the surfaces. There is no reason to distinguish between their positive and negative sides.

(c) Boundaries of the computational volume. The coordinate planes (surfaces) forming the boundaries of the computational volume may be indexed as follows: 101 for $x^1 - x^1_{\mathrm{MIN}} = 0$, 102 for $x^1 - x^1_{\mathrm{MAX}} = 0$, 103 for $x^2 - x^2_{\mathrm{MIN}} = 0$, 104 for $x^2 - x^2_{\mathrm{MAX}} = 0$, 105 for $x^3 - x^3_{\mathrm{MIN}} = 0$, and 106 for $x^3 - x^3_{\mathrm{MAX}} = 0$.

(d) Isochrone $\tau - \tau_{\mathrm{MAX}} = 0$. The isochrone may be indexed by 107.

For determination of the surfaces for storage, the indices of the surfaces forming the set F_{STORE} must be specified and a subroutine SRFC2 must be available to evaluate the functions $f(x^i)$ that describe the proper surfaces. Remember that the indices of the surfaces covering interfaces must be supplemented by a $\pm$ sign denoting the side of the surface where the quantities are to be stored.

Each surface used for storage should have its own file with stored quantities.

5.5.3 Storage of quantities at the endpoints of rays of elementary waves

Each elementary wave is defined by means of its code (see Section 4). Left-hand parts of the code usually define some simpler elementary waves, with a smaller number of elements of their rays. It may be useful to store quantities corresponding to these simpler elementary waves at the endpoints of their rays. These quantities may be used in the computation of other elementary waves, with longer chains of elements, but with the same initial elements. Their computation may start from the

stored quantities, without repeating the computation of the initial elements.

5.5.4 List of stored quantities

In addition to quantities computed along a ray and described in Section 5.2, some quantities describing local properties of the model at points under consideration along the ray may be useful in further processing of the results of complete ray tracing. These quantities, which will already have been evaluated during complete ray tracing, can, in principle, be recomputed when required. This may, however, be rather time-consuming. It is therefore reasonable to store these quantities together with quantities computed along the ray. The additional (local) quantities to be stored are:

ICB1	index of the complex block in which the point is situated, including the sign + for a P wave or − for an S wave;
$YL(1) = v_P$	velocity of P waves at the point;
$YL(2) = v_S$	velocity of S waves at the point;
$YL(3) = \rho$	density at the point;
$YL(4) = v_1 = \partial v/\partial x^1$ $YL(5) = v_2 = \partial v/\partial x^2$ $YL(6) = v_3 = \partial v/\partial x^3$	velocity derivatives in general coordinates.

After these local quantities, the quantities Y(1), . . . , Y(NY) described in Section 5.2 are to be stored.

If the quantities are stored at a point of intersection of the ray with a specified surface, and if the surface coincides with an interface between blocks (i.e. the surface belongs to the set of NSRFC surfaces covering interfaces) then the quantities ICB1, YL and Y should be stored not only once, but either for three waves (incident, reflected P, reflected S) or for two waves (transmitted P, transmitted S), depending on the side of the surface where they are stored.

In certain applications, it may also be sufficient to replace the above three or two sets of quantities by a single set of quantities corresponding to the incident wave. However, in this case the reduced amplitudes Y(28), . . . , Y(NY) in the ray-centred coordinate system should be replaced by reduced amplitudes involving appropriate conversion coefficients,

expressed in ray-centred coordinates:

(a) P wave at the initial point (6 reals):

$$\begin{aligned} \mathrm{YC}(1) &= \mathrm{Re}\, A_{13}, & \mathrm{YC}(2) &= \mathrm{Im}\, A_{13}, \\ \mathrm{YC}(3) &= \mathrm{Re}\, A_{23}, & \mathrm{YC}(4) &= \mathrm{Im}\, A_{23}, \\ \mathrm{YC}(5) &= \mathrm{Re}\, A_{33}, & \mathrm{YC}(6) &= \mathrm{Im}\, A_{33}. \end{aligned}$$

(b) S wave at the initial point (12 reals):

$$\begin{aligned} \mathrm{YC}(1) &= \mathrm{Re}\, A_{11}, & \mathrm{YC}(2) &= \mathrm{Im}\, A_{11}, \\ \mathrm{YC}(3) &= \mathrm{Re}\, A_{21}, & \mathrm{YC}(4) &= \mathrm{Im}\, A_{21}, \\ \mathrm{YC}(5) &= \mathrm{Re}\, A_{31}, & \mathrm{YC}(6) &= \mathrm{Im}\, A_{31}, \\ \mathrm{YC}(7) &= \mathrm{Re}\, A_{12}, & \mathrm{YC}(8) &= \mathrm{Im}\, A_{12}, \\ \mathrm{YC}(9) &= \mathrm{Re}\, A_{22}, & \mathrm{YC}(10) &= \mathrm{Im}\, A_{22}, \\ \mathrm{YC}(11) &= \mathrm{Re}\, A_{32}, & \mathrm{YC}(12) &= \mathrm{Im}\, A_{32}. \end{aligned}$$

5.6 Data for complete ray tracing

In this section we summarize the input data necessary for the complete ray tracing (in addition to those discussed in Sections 2, 3, 4 and 6).

(a) The coordinates x^1_{MIN}, x^1_{MAX}, x^2_{MIN}, x^2_{MAX}, x^3_{MIN}, x^3_{MAX}, which specify the coordinate planes bounding the computational volume, and the maximum travel time τ_{MAX}. The coordinate planes may be indexed 101, 102, 103, 104, 105, 106. Boundaries of the model (see Section 3.2.1) may be used as default surfaces for the coordinate planes bounding the computational volume.

(b) The number NSRFCA of auxiliary surfaces. The surfaces are indexed sequentially by positive integers, from NSRFC + 1 to NSRFC + NSRFCA.

(c) The indices of end surfaces (model or auxiliary surfaces bounding the computational volume—see Section 5.4f). The surfaces described by data (a) need not be specified in this set of indices. The indices may be specified in an arbitrary order.

(d) The indices of surfaces for storing computed quantities (see Section 5.5.2). The indices may be specified in an arbitrary order. The indices of surfaces 1, . . . , NSRFC covering structural interfaces should include a sign + or − (see Section 5.5.2a).

(e) Integer KSTORE specifying whether conversion coefficients are to be considered.

(f) Exponent NEXPS specifying independent variable along rays—see (5.1).

(g) Maximum allowed number NHLF of halvings (bisections) of initial increment of independent variable during numerical integration.

(h) Step STORE of independent variables for storing the computed quantities along a ray (see Section 5.5.1). For STORE = 0 the quantities are not stored along rays.

(i) Initial increment $\Delta\sigma = \text{STEP}$ of independent variable for numerical integration.

(j) Upper error bound UEB of travel time per step of numerical integration. Errors in the coordinates of points along the ray are approximately transformed to units of travel time and are also bounded by UEB. The error per step of numerical integration is automatically kept within the limit UEB if this does not require more than NHLF bisections of the initial increment STEP. In the opposite case the upper error bound is $2, 4, 8, \ldots$ times greater for the computation of the rest of the ray. Thus the computation of each ray is completed.

(k) The maximum allowed accumulated deviations UEBPP, UEBPH, UEBHH of the two computed polarization vectors from the conditions of orthonormality (see Sections 5.8.2d and 5.8.3i). The accumulated deviations (quantities YY(3), YY(4), YY(5) defined in Section 5.2.2) may be compared with the specified limits UEBPP, UEBPH, UEBHH. The maximum accumulated deviations UEBPP, UEBPH, UEBHH are expressed in time units.

(l) The maximum allowed deviation UEBDRT of the matrix $\boldsymbol{\Pi}^{\mathrm{T}}\boldsymbol{\Sigma}\boldsymbol{\Pi}$ from the matrix

$$\boldsymbol{\Sigma} = \begin{bmatrix} 0 & 0 & 1 & 0 \\ 0 & 0 & 0 & 1 \\ -1 & 0 & 0 & 0 \\ 0 & -1 & 0 & 0 \end{bmatrix};$$

see (5.11). A deviation of any component may be compared with the specified limit UEBDRT.

5.7 Complete ray tracing

We assume the model (Section 3), the input data for complete ray tracing (Section 5.6) and the code of the elementary wave (Section 4) to be specified. If the quantities $Y(1), \ldots, Y(NY)$, $YY(1), \ldots, YY(5)$, $IY(1), \ldots, IY(12)$, Q_{AB}^{INIT} and P_{AB}^{INIT} (see Section 5.2) are given then the complete ray tracing of the ray of the specified elementary wave may continue from the given point Y(3), Y(4), Y(5).

(a) If the point is situated inside a complex block then computation of the ray continues as described in Section 5.8, until the endpoint of the computed element of the ray is reached (the endpoint of the element is either the endpoint of the ray (see Section 5.4) or the point of intersection of the ray with the boundary of the complex block).

(b) If the point is the endpoint of the element of the ray, situated at the boundary of a complex block, then: if the index IY(6) = ISRF of the surface is specified in the input data for storing the computed quantities (see Section 5.6d), the proper quantities (see Section 5.5.4) are stored in the file corresponding to the surface. If the surface is the end surface (see Section 5.6c) then the computation of the ray is terminated (see Sections 5.4d–f), or else the quantities $Y(1), \ldots, Y(NY)$, $YY(1), \ldots, YY(5)$, $IY(1), \ldots, IY(12)$ must be transformed across the interface. The code for the elementary wave specifies whether the ray is to be transmitted or reflected and whether it has to continue as a P or an S wave. Transformation of the quantities across the interface is described in Section 5.9. Note that also the subroutine CODE (see Section 4) for the interpretation of the code may indicate the endpoint of the ray (see Sections 5.4a, b(i)–b(iii)). Similarly, the subroutine for the transformation at an interface (Section 5.9) may indicate the endpoint of the ray (see Sections 5.4b(iv), b(v), c). After transformation, the computation of the ray continues as described in Section 5.8, until the endpoint of the computed element of the ray is reached.

To start complete ray tracing at the initial point of a ray, the quantities $Y(1), \ldots, Y(NY)$, $YY(1), \ldots, YY(5)$, $IY(1), \ldots, IY(12)$, Q_{AB}^{INIT} and P_{AB}^{INIT} must be specified at the initial point of the ray. The specification of the above quantities at the initial point of the ray is discussed in Section 6.

5.8 Complete ray tracing through a complex block

The element of a ray situated inside a complex block ICB1 is computed by means of numerical integration of the system of 27 ordinary

differential equations (5.2)–(5.4) and (5.6) for $J = 1$ and (5.9). The standard subroutines HPCG or RKGS from the IBM Scientific Subroutine Package may be used for the integration. In HPCG the solution of ordinary differential equations is evaluated by means of Hamming's modified predictor–corrector method, which is a fourth-order method. RKGS uses the Runge–Kutta method (also a fourth-order method). Routine HPCG needs two evaluations of the right-hand sides of differential equations per step of the integration, but its starting takes approximately 18 additional evaluations. Routine RKGS needs 11 evaluations of right-hand sides of differential equations per two steps of the integration. Thus HPCG should be usually more effective than RKGS, but for short elements of a ray (up to four steps of numerical integration) RKGS may be more effective.

The numerical computation of the element of a ray situated inside a complex block is organized by a routine called RAYCB here (see Section 5.8.1).

The right-hand sides of the ordinary differential equations are evaluated by SUBROUTINE FCT(X, Y, D) (see Section 5.8.2).

The necessary tests and auxiliary computations performed after each successful step of numerical integration are carried out in SUBROUTINE OUTP(X, Y, D, IHLF, NDIM, PRMT) (see Section 5.8.3).

5.8.1 *A short description of complete ray tracing through one block*

The subroutine RAYCB transfers the quantities given at the initial point of the element of a ray into the corresponding quantities at the endpoint of the element.

The quantities are Y(1), . . . , Y(NY), described in Section 5.2.1, and the auxiliary quantities YY(1), . . . , YY(5), IY(1), . . . , IY(12), described in Section 5.2.2. The auxiliary quantities IY(2) = KODIND and IY(3) = ICB0 are not required by the routine RAYCB, the quantities IY(6) = ISRF, IY(7) = ISB2 and IY(8) = ICB2 are only output parameters.

The endpoint of the element is the next point of intersection of the ray with a boundary of the computational volume, with a boundary of the complex block ICB1, or with an end surface (see Section 5.4). The index of the crossed surface is stored in IY(6) = ISRF. If the interface between two complex blocks is crossed then the indices of the simple and complex blocks situated on the other side of the interface are stored in IY(7) = ISB2 and IY(8) = ICB2.

The quantities Y(1), . . . , Y(27) are computed by

```
SUBROUTINE HPCG (PRMT, Y, DERY, NDIM, IHLF, FCT, OUTP, AUX)
REAL PRMT(5), Y(NDIM), DERY(NDIM), AUX(16, NDIM)
INTEGER NDIM, IHLF
```

or by

```
SUBROUTINE RKGS (PRMT, Y, DERY, NDIM, IHLF, FCT, OUTP, AUX)
REAL PRMT(5), Y(NDIM), DERY(NDIM), AUX(8, NDIM)
INTEGER NDIM, IHLF
```

respectively, FCT and OUTP being external subroutines in both cases.

The meaning of individual parameters is described in detail in the IBM Scientific Subroutine Package, we shall not repeat it here. We shall only give the specification of these parameters in our case of complete ray tracing.

The right-hand sides of the ordinary differential equations are evaluated by the subroutine FCT. The routine OUTP, called by HPCG (or RKGS) after every successful step, looks for the endpoint of the computed element, controls the phase shift of the reduced amplitudes Y(28), . . . , Y(NY) due to caustics, and stores the computed quantities inside the complex block in proper files. The communication among the subroutines RAYCB, FCT and OUTP is performed by the local common block /RAYC/.

Structure and function of the routine RAYCB

(a) The input auxiliary quantities (see Section 5.2.2) are stored in the common block /RAYC/.

(b) The interval of the independent variable S for the numerical integration extends from PRMT(1) = YY(1) to a sufficiently large value (e.g. PRMT(2) = PRMT(1) + 999 999). The initial increment of the independent variable is PRMT(3) = $\Delta\sigma$ = STEP (see Section 5.6). The upper error bound is PRMT(4) = 13.444 × UEBRAY for HPCG or PRMT(4) = UEBRAY for RKGS. The parameter PRMT(5) controls the termination of numerical integration and need not be specified. Error weights may be selected for example as follows:

for real and imaginary parts of a complex-valued travel time

$$\text{DERY}(1) = 1, \qquad \text{DERY}(2) = 1;$$

for coordinates

$$\mathrm{DERY}(3) = \frac{(G_{11})^{1/2}}{v}, \qquad \mathrm{DERY}(4) = \frac{(G_{22})^{1/2}}{v},$$

$$\mathrm{DERY}(5) = \frac{(G_{33})^{1/2}}{v};$$

for covariant components of the slowness vector

$$\mathrm{DERY}(6) = (G^{11})^{1/2}\,\Delta\sigma\, v^{1-\mathrm{NEXPS}},$$
$$\mathrm{DERY}(7) = (G^{22})^{1/2}\,\Delta\sigma\, v^{1-\mathrm{NEXPS}},$$
$$\mathrm{DERY}(8) = (G^{33})^{1/2}\,\Delta\sigma\, v^{1-\mathrm{NEXPS}};$$

for other computed quantities

$$\mathrm{DERY}(I) = 0 \quad \text{for } I = 9, \ldots, 27.$$

The velocity v of the corresponding type of wave and the components G^{ij} and G_{ij} of the metric tensor are taken at the point where the numerical integration starts, they represent approximately the values of the velocity and the metric tensor along the computed part of the ray. Note that only approximate values of these quantities are needed at this place; they control only the error weights, not the actual computations.

(c) The routine HPCG (or RKGS) is called.

(d) The value of the independent variable at the endpoint of the computed element of the ray is copied from the common block /RAYC/ to the variable YY(1). If the numerical integration is interrupted for a great number of bisections of the initial increment (greater than NHLF, i.e. PRMT(5) < 0, see Section 5.8.3j) then the upper error bound UEBRAY is doubled and the algorithm continues again from (b).

(e) The auxiliary quantities (see Section 5.2.2) are recalled from the common block /RAYC/ to proper arrays.

5.8.2 *Right-hand sides of the differential equations (subroutine FCT)*

In this section we shall describe the algorithm for evaluating the right-hand sides of the system of 27 ordinary differential equations for Y(1), . . . , Y(27); see (5.2)–(5.4) and (5.6) for $J = 1$ and (5.9). We assume that the algorithm is realized by the routine FCT, by the following steps (a)–(g).

(a) The number IFCT of invocations of FCT (see Section 5.2.2) is increased by one.

(b) The components G^{ij} of the metric tensor and Christoffel symbols Γ^k_{ij} are determined using the routine METRIC (see Section 2.1). The velocity v, its derivatives $\partial v/\partial x^i$ and $\partial^2 v/\partial x^i\,\partial x^j$, and the loss factor Q^{-1} are determined using the routine VELOC (see Section 3.3.2).

(c) The basis of the ray-centred coordinate system and some related quantities are determined as follows:

(i) non-unit vectors

$$p_i = \mathrm{Y}(i+5), \qquad H_{i1} = \mathrm{Y}(i+8);$$

(ii) contravariant components

$$p^i = G^{ij}p_j, \qquad H^{i1} = G^{ij}H_{j1};$$

(iii) norms

$$d_{11} = (H^{i1}H_{i1})^{1/2}, \qquad d_{33} = (p^i p_i)^{1/2}, \qquad d_{13} = \frac{p^i H_{i1}}{d_{11}d_{33}};$$

(iv) orthonormal vectors

$$H_{i3} = \frac{p_i}{d_{33}}, \qquad H^{i3} = \frac{p^i}{d_{33}},$$

$$H_{i1} = \frac{H_{i1}}{d_{11}} - H_{i3}d_{13}, \qquad H^{i1} = \frac{H^{i1}}{d_{11}} - H^{i3}d_{13},$$

$$H_{i2} = (\det G^{rs})^{-1/2}\varepsilon_{ijk}H^{j3}H^{k1}, \qquad H^{i2} = G^{ij}H_{j2}.$$

(d) Quantities useful to test the accuracy of computations: for exact solutions, the norms d_{11}, d_{33}, d_{13} introduced above should be as follows: $d_{11} = 1$, $d_{33} = v^{-1}$, $d_{13} = 0$. The deviations

$$\Delta_{11} = |d_{11} - 1|, \qquad \Delta_{33} = |vd_{33} - 1|, \qquad \Delta_{13} = |d_{13}|$$

of the basis of the ray-centred coordinate system from the orthonormality conditions are stored in the common block /RAYC/ in order to be accumulated along the whole ray by means of routine OUTP. The accumulated values are useful to check the accuracy of the numerical integration.

(e) First and second derivatives of the velocity in the ray-centred coordinate system:

$$V_1 = \frac{\partial v}{\partial x^i}H^{i1}, \qquad V_{AB} = \left(\frac{\partial^2 v}{\partial x^i\,\partial x^j} - \Gamma^k_{ij}\frac{\partial v}{\partial x^k}\right)H^{iA}H^{jB}.$$

(f) Correction of the computed quantities (i.e. renormalization of the slowness vector and of the first polarization vector):

$$\mathrm{Y}(i+5) = H_{i3}/v, \qquad \mathrm{Y}(i+8) = H_{i1}.$$

(g) Right-hand sides of the differential equations

$$\frac{\mathrm{d}\tau}{\mathrm{d}\sigma} = v^{-\mathrm{NEXPS}}, \qquad \frac{\mathrm{d}\tau^{\mathrm{IM}}}{\mathrm{d}\sigma} = \tfrac{1}{2}Q^{-1}v^{-\mathrm{NEXPS}},$$

$$\frac{\mathrm{d}x^i}{\mathrm{d}\sigma} = H^{i3}v^{1-\mathrm{NEXPS}},$$

$$\frac{\mathrm{d}p_i}{\mathrm{d}\sigma} = \left(-v^{-1}\frac{\partial v}{\partial x^i} + \Gamma^k_{ij}H^{j3}H_{k3}\right)v^{-\mathrm{NEXPS}},$$

$$\frac{\mathrm{d}H_{i1}}{\mathrm{d}\sigma} = (V_1 H_{i3} + v\Gamma^k_{ij}H^{j3}H_{k1})v^{-\mathrm{NEXPS}},$$

$$\frac{\mathrm{d}\Pi_{\alpha\beta}}{\mathrm{d}\sigma} = v^{-1-\mathrm{NEXPS}}\begin{bmatrix} 0 & 0 & v^3 & 0 \\ 0 & 0 & 0 & v^3 \\ -V_{11} & -V_{12} & 0 & 0 \\ -V_{12} & -V_{22} & 0 & 0 \end{bmatrix} \times \begin{bmatrix} \mathrm{Y}(12) & \mathrm{Y}(16) & \mathrm{Y}(20) & \mathrm{Y}(24) \\ \mathrm{Y}(13) & \mathrm{Y}(17) & \mathrm{Y}(21) & \mathrm{Y}(25) \\ \mathrm{Y}(14) & \mathrm{Y}(18) & \mathrm{Y}(22) & \mathrm{Y}(26) \\ \mathrm{Y}(15) & \mathrm{Y}(19) & \mathrm{Y}(23) & \mathrm{Y}(27) \end{bmatrix}.$$

5.8.3 Subroutine OUTP

The routine OUTP is called by HPCG (or RKGS) after any successful step of the numerical integration. It includes various tests of the position of the newly computed point of the ray, tests for possible caustic points, etc. It also stores the computed quantities in proper files if required. The detailed step-to-step description of the algorithm is as follows.

(a) The values of the independent variable X, dependent variables Y and their derivatives D, stored one step before in the variable X2 and in arrays Y2(NY), D2(NY), are moved into X1 and into arrays Y1 and D1. The input values of the parameters X, Y, D of the subroutine OUTP are copied to X2 and to arrays Y2, D2. The variable X2 and arrays Y2, D2 are located in the common block /RAYC/, since their values must be saved until the next invocation of OUTP.

At the beginning of the numerical integration (i.e. if the independent variable X equals PRMT(1)), return to HPCG (or to RKGS).

(b) The number IY(10) = IOUTP (see Section 5.2.2) of steps of numerical integration of the ray is increased by 1. The index IY(6) = ISRF of a surface is set equal to zero.

(c) *Check for crossing the coordinate boundaries of the computational volume.* The boundaries are described by seven reals (see Section 5.6). If any one of the seven limits (indexed from 101 to 107) is exceeded, i.e. if any one of $f_{2i+99} = x^i - x^i_{\mathrm{MIN}}$ is less or equal to zero, or if any one of $f_{2i+100} = x^i - x^i_{\mathrm{MAX}}$ is greater or equal to zero, or if $f_{107} = \tau - \tau_{\mathrm{MAX}}$ is greater or equal to zero, then: the index ISRF is set equal to the relevant index from 101 to 107 and the point of intersection is sought. The point of intersection is situated on the ray Ω between X1, Y1 and X, Y. The independent variable X and dependent variables Y are replaced by the values at the point of intersection. The point of intersection may be found by means of the procedure described in Section 5.8.4. Note that the gradients of the functions $f_{101}, \ldots, f_{107}$ are as follows:

$$\frac{\partial f_{2k+99}}{\partial x^j} = \frac{\partial f_{2k+100}}{\partial x^j} = \begin{cases} 1 & \text{for } k = 1, 2, 3, j = k, \\ 0 & \text{for } k = 1, 2, 3, j \neq k, \end{cases}$$

$$\frac{\partial f_{107}}{\partial x^j} = p_j.$$

(d) *Check for crossing the boundary of the complex block.* The indices of the simple and complex blocks in which the point X, Y is situated may be obtained by invocation of the subroutine BLOCK (see Section 3.3.1). If the ray has not left the complex block IY(5) = ICB1 (i.e. if the index of the complex block is equal to ICB1) then the value of IY(4) = ISB1 is replaced by the index of the current simple block. Otherwise (if the ray has left the complex block ICB1), the point of intersection of the ray with the boundary of the complex block ICB1 must be found as follows.

(d_1) The independent variable X is copied to an auxiliary variable XAUX and the coordinates Y(3), . . . , Y(5) are copied to an auxiliary array YAUX.

(d_2) IY(6) = ISRF is set equal to the index of the surface that separates the point X, Y from the simple block ISB1.

(d_3) The point X, Y of intersection of the ray with the surface ISRF is found by means of the procedure described in Section 5.8.4. The subroutine BLOCK is called to find the simple and complex blocks IY(7) = ISB2 and IY(8) = ICB2 touching at the point X, Y of intersection the simple block ISB1 from the other side of the surface ISRF. Then there are three possibilities.

(i) The point X, Y of intersection is separated from the simple block ISB1 by a surface bounding ISB1. This means that the point X, Y is not situated at the boundary of the simple block ISB1. The algorithm must be repeated starting from (d_2).

(ii) Otherwise, if the neighbouring complex block ICB2 is equal to ICB1, the point X, Y is situated at the boundary between two simple blocks, but not at the boundary of the complex block ICB1. The value ISB1 must be replaced by ISB2 and the subroutine BLOCK must be called to find the new surface ISRF separating the point XAUX, YAUX from the simple block ISB1. The algorithm must be repeated starting from (d_3). Note that the point of intersection will be situated between X1, Y1 and X = XAUX, Y = YAUX.

(iii) Otherwise, the point X, Y of intersection is successfully found.

(e) *Check for crossing the end surfaces.* All surfaces on which complete ray tracing should be terminated and that are different from the surfaces 1, . . . , NSRFC covering structural interfaces must be checked for crossing. If the point X, Y is situated on the other side from an end surface than the initial point of the ray, then IY(6) = ISRF is set equal to the index of the surface and the point of intersection is found. The values at the point are stored in variable X and array Y.

(f) *Phase shift due to caustics.* The matrix Q^{R}_{AB} of geometrical spreading is dependent on the matrix Q^{INIT}_{AB} of geometrical spreading and its derivative P^{INIT}_{AB} at the initial point of the ray (see Sections 5.1.3 and 5.2.3):

$$\begin{bmatrix} Q^{\mathrm{R}}_{11} & Q^{\mathrm{R}}_{12} \\ Q^{\mathrm{R}}_{21} & Q^{\mathrm{R}}_{22} \end{bmatrix} = \begin{bmatrix} \Pi_{11} & \Pi_{12} & \Pi_{13} & \Pi_{14} \\ \Pi_{21} & \Pi_{22} & \Pi_{23} & \Pi_{24} \end{bmatrix} \begin{bmatrix} Q^{\mathrm{INIT}}_{11} & Q^{\mathrm{INIT}}_{12} \\ Q^{\mathrm{INIT}}_{21} & Q^{\mathrm{INIT}}_{22} \\ P^{\mathrm{INIT}}_{11} & P^{\mathrm{INIT}}_{12} \\ P^{\mathrm{INIT}}_{21} & P^{\mathrm{INIT}}_{22} \end{bmatrix}.$$

The matrices Q_{AB}^{INIT} and P_{AB}^{INIT} are stored in the array YI (see Section 6.1). We denote

$$\begin{bmatrix} Q_{11}^1 & Q_{12}^1 \\ Q_{21}^1 & Q_{22}^1 \end{bmatrix} = \begin{bmatrix} \mathrm{Y1(12)} & \mathrm{Y1(16)} & \mathrm{Y1(20)} & \mathrm{Y1(24)} \\ \mathrm{Y1(13)} & \mathrm{Y1(17)} & \mathrm{Y1(21)} & \mathrm{Y1(25)} \end{bmatrix} \times \begin{bmatrix} \mathrm{YI(12)} & \mathrm{YI(16)} \\ \mathrm{YI(13)} & \mathrm{YI(17)} \\ \mathrm{YI(14)} & \mathrm{YI(18)} \\ \mathrm{YI(15)} & \mathrm{YI(19)} \end{bmatrix},$$

the matrix of geometrical spreading at the point X1, Y1. Similarly we denote

$$\begin{bmatrix} Q_{11}^2 & Q_{12}^2 \\ Q_{21}^2 & Q_{22}^2 \end{bmatrix} = \begin{bmatrix} \mathrm{Y(12)} & \mathrm{Y(16)} & \mathrm{Y(20)} & \mathrm{Y(24)} \\ \mathrm{Y(13)} & \mathrm{Y(17)} & \mathrm{Y(21)} & \mathrm{Y(25)} \end{bmatrix} \times \begin{bmatrix} \mathrm{YI(12)} & \mathrm{YI(16)} \\ \mathrm{YI(13)} & \mathrm{YI(17)} \\ \mathrm{YI(14)} & \mathrm{YI(18)} \\ \mathrm{YI(15)} & \mathrm{YI(19)} \end{bmatrix},$$

the matrix of geometrical spreading at the point X, Y.

If

$$\det \boldsymbol{Q}^1 \det \boldsymbol{Q}^2 < 0,$$

where $\det \boldsymbol{Q}^1 = Q_{11}^1 Q_{22}^1 - Q_{12}^1 Q_{21}^1$ and $\det \boldsymbol{Q}^2 = Q_{11}^2 Q_{22}^2 - Q_{12}^2 Q_{21}^2$, then there is a caustic point of first order (line caustic) between the points X1, Y1 and X, Y. Then the reduced amplitudes Y(28), . . . , Y(NY) must be multiplied by $-\mathrm{i}$, and IY(12) = KMAH is increased by one.

Otherwise, if

$$(Q_{11}^1 Q_{22}^2 - Q_{12}^1 Q_{21}^2 + Q_{22}^1 Q_{11}^2 - Q_{21}^1 Q_{12}^2) \det \boldsymbol{Q}^1 < 0$$

then there is a caustic point of second order (point caustic) between points X1, Y1 and X, Y. Then the reduced amplitudes Y(28), . . . , Y(NY) must change their signs, and IY(12) = KMAH is increased by two.

(g) *Storage of the computed quantities at given surfaces.* The loop over all surfaces specified for storage of the computed quantities, and different from the surfaces 1, . . . , NSRFC covering interfaces, must be performed. If a surface is identical with the surface ISRF on which the endpoint X, Y of the element is situated then the

quantities at this point are stored in the corresponding file (see Section 5.5.2). Otherwise, if the point X, Y is situated on the other side from the surface from the point X1, Y1 then the point of intersection of the ray with the surface is found and the independent variable and the dependent variables at the point are temporarily stored in the auxiliary variable XAUX and auxiliary array YAUX. The reduced amplitudes YAUX(28), . . . , YAUX(NY) are obtained from the amplitudes Y(28), . . . , Y(NY) by adding the phase shift due to the caustics between the points X, Y and XAUX, YAUX. The phase shift may be determined in the same way as described in (f). We must remember, however, that the point XAUX, YAUX is situated against the direction of propagation from the point X, Y. Then a factor i must be used instead of $-$i in (f).

(h) *Storage of computed quantities along the ray.* The quantities are stored along the ray with the given step STORE (see Section 5.6h) in the independent variable if STORE $\neq 0$. We denote

$$k_1 = \text{int}\,(\text{X1/STORE}) + 1, \qquad k_2 = \text{int}\,(\text{X/STORE}).$$

The quantities are stored at the points given by the following values of the independent variable:

$$\text{XAUX} = k \times \text{STORE} \quad (k = k_1, \ldots, k_2).$$

For $k_1 > k_2$ the data are not stored. The dependent variables YAUX(1), . . . , YAUX(27) at the point XAUX may be obtained by interpolation from the points X1, Y1 and X2, Y2. The interpolation method is described in Section 5.8.4. The reduced amplitudes YAUX(28), . . . , YAUX(NY) may be obtained in the same way as in (g).

(i) *Accumulation of the renormalization errors for a test of accuracy.* The quantities Δ_{33}, Δ_{13} and Δ_{11} (see Section 5.8.2d), stored in the common block /RAYC/, are multiplied by $\frac{1}{2}(\text{X} - \text{X1})v^{-\text{NEXPS}}$ and are added to the quantities YY(3) = ERRPP, YY(4) = ERRPH, YY(5) = ERRHH (see Section 5.2.2), temporarily stored in the common block /RAYC/.

(j) *Large number of bisections of the initial step.* If the number IHLF of bisections is greater than the given limit NHLF then the numerical integration is interrupted by setting PRMT(5) negative (numerical integration is interrupted for PRMT(5) non-zero).

(k) *Final operations.* The value X of the independent variable is stored in the common block /RAYC/. If ISRF $\neq 0$ (i.e. the endpoint of the element of the ray is reached) then the numerical integration is terminated by setting PRMT(5) positive.

5.8.4 Auxiliary procedures

In the routine OUTP it is necessary to perform the interpolation of certain quantities along the ray, and to find the points of intersection of the ray with certain given surfaces. The algorithms for the solution of these two problems are described in this section.

(a) Interpolation along the ray

The part of the ray between two consequent points obtained by numerical integration may be interpolated by a third-order method using the functional values and their first derivatives at the two points. We denote by x_1, y_1, y_1' (x_2, y_2, y_2') the independent variable, the dependent variables and their derivatives in the first (second) of the two given points. We introduce four functions of the independent variable x:

$$\begin{aligned} a_1(x) &= [2a(x)+3]a(x)a(x), \\ a_2(x) &= 1 - a_1(x), \\ b_1(x) &= [a(x)+1]a(x)(x-x_2), \\ b_2(x) &= [a(x)+1]a(x)(x-x_1), \end{aligned}$$

where

$$a(x) = (x-x_2)/(x_2-x_1).$$

They have the following properties:

$$\begin{bmatrix} a_1(x_1) & a_1(x_2) & a_1'(x_1) & a_1'(x_2) \\ a_2(x_1) & a_2(x_2) & a_2'(x_1) & a_2'(x_2) \\ b_1(x_1) & b_1(x_2) & b_1'(x_1) & b_1'(x_2) \\ b_2(x_1) & b_2(x_2) & b_2'(x_1) & b_2'(x_2) \end{bmatrix} = \begin{bmatrix} 1 & 0 & 0 & 0 \\ 0 & 1 & 0 & 0 \\ 0 & 0 & 1 & 0 \\ 0 & 0 & 0 & 1 \end{bmatrix}.$$

Here the functions

$$\begin{aligned} a_1'(x) &= 6[a(x)+1]a(x)/(x_2-x_1), \\ a_2'(x) &= -a_1'(x), \\ b_1'(x) &= [3a(x)+2]a(x), \\ b_2'(x) &= [3a(x)+1][a(x)+1], \end{aligned}$$

are the first derivatives of the functions $a_1(x)$, $a_2(x)$, $b_1(x)$ and $b_2(x)$. The values of the dependent variables and their derivatives at x are then determined by

$$y = a_1 y_1 + a_2 y_2 + b_1 y_1' + b_2 y_2',$$
$$y' = a_1'(y_1 - y_2) + b_1' y_1' + b_2' y_2'.$$

(b) The search for the intersection of the ray with a given surface

The search for the point of intersection of a ray parametrized by an independent variable X with a surface $f(x^i) = 0$ is started if

$$f(x^i(\mathrm{XA}))f(x^i(\mathrm{XB})) < 0$$

for two points XA, XB of the ray. The point of intersection must be situated between XA and XB.

The ray is interpolated between its two last points obtained by numerical integration using the third-order method described in (a). The function $f(x^i)$ is evaluated by means of the subroutine SRFC2 if the index ISRF of the surface is less than 100. For ISRF > 100 the functions $f_{101}, \ldots, f_{107}$ are used.

The point of intersection can be found iteratively by a combined two-point method. The *regula falsi* method is used in each odd iteration, the Newton–Raphson method in each even iteration. Since the Newton–Raphson method need not converge, it is replaced by the method of bisections in the case of emergency. The last approximation of X is taken for a new XB. That one of the old XA, XB at which the function $f(x^i)$ has the opposite sign to $f(x^i(X))$ is taken for a new XA. The iterations are terminated if the new interval $\langle \mathrm{XA}, \mathrm{XB} \rangle$ of the independent variable is sufficiently small:

$$|\mathrm{XA} - \mathrm{XB}| \leqslant \mathrm{ERR},$$

with

$$\mathrm{ERR} = \mathrm{UEB}\ v^{-\mathrm{NEXPS}},$$

where v is the velocity of propagation of the corresponding type of wave.

The *regula falsi* iteration (odd iteration) is as follows:

$$\mathrm{X} = (\mathrm{FA} \times \mathrm{XB} - \mathrm{FB} \times \mathrm{XA})/(\mathrm{FA} - \mathrm{FB}),$$

where

$$\mathrm{FA} = f(x^i(\mathrm{XA})), \qquad \mathrm{FB} = f(x^i(\mathrm{XB})).$$

The modified Newton–Raphson iteration (even iteration) is as follows.

We denote

$$\begin{aligned} \mathrm{XC} &= (\mathrm{XA} + \mathrm{XB})/2, \\ \mathrm{XCA} &= \mathrm{XA} - \mathrm{FA}/\mathrm{DA} + (\mathrm{ERR}/50)\,\mathrm{sign}\,(\mathrm{XA} - \mathrm{XB}), \\ \mathrm{XCB} &= \mathrm{XB} - \mathrm{FB}/\mathrm{DB} + (\mathrm{ERR}/50)\,\mathrm{sign}\,(\mathrm{XA} - \mathrm{XB}), \end{aligned}$$

where

$$\mathrm{DA} = \frac{\partial f}{\partial x^k}(x^i(\mathrm{XA}))\,\frac{\partial x^k}{\partial X}(\mathrm{XA}), \qquad \mathrm{DB} = \frac{\partial f}{\partial x^k}(x^i(\mathrm{XB}))\,\frac{\partial x^k}{\partial X}(\mathrm{XB}).$$

If XCA and XCB are situated between points XB and XC then

$$\mathrm{X} = \begin{cases} \mathrm{XCA} & \text{for } |\mathrm{XCA} - \mathrm{XB}| < |\mathrm{XCB} - \mathrm{XB}|, \\ \mathrm{XCB} & \text{for } |\mathrm{XCB} - \mathrm{XB}| \leqslant |\mathrm{XCA} - \mathrm{XB}|. \end{cases}$$

If only XCA is situated between XB and XC then

$$\mathrm{X} = \mathrm{XCA}.$$

If only XCB is situated between XB and XC then

$$\mathrm{X} = \mathrm{XCB}.$$

If neither XCA nor XCB is situated between XB and XC then

$$\mathrm{X} = \mathrm{XC}.$$

5.9 Complete ray tracing across a curved interface

The quantities Y(1), . . . , Y(NY), YY(1), . . . , YY(5) and IY(1), . . . , IY(12) computed along a ray and defined in Section 5.2 must be transformed at an interface. We denote the quantities Y, YY, IY (described in Section 5.2) corresponding to the incident wave and the reflected/transmitted wave at the point of incidence by Y1, YY1, IY1 and Y2, YY2, IY2 respectively. We also denote by KODNEW the new position in the code, and by |ICBNEW| the index of the complex block in which the generated wave is to propagate. The sign of ICBNEW specifies the type of generated wave (+ for P, − for S).

5.9.1 Transformation of auxiliary quantities, travel time and coordinates

(a) The number of real-valued quantities describing the reduced amplitudes of the incident wave is NAMPL1 = IY1(1) − 27.

(b) The number NAMPL2 of real-valued quantities specifying the reduced amplitudes of the generated wave is
  (b_1) if IY1(5) > 0 and ICBNEW < 0 then NAMPL2 = 2 NAMPL1;
  (b_2) if IY1(5) < 0 and ICBNEW > 0 then NAMPL2 = NAMPL1/2;
  (b_3) otherwise NAMPL2 = NAMPL1.

(c) The output number of basic quantities is IY2(1) = 27 + NAMPL2.

(d) The new position in the code is IY2(2) = KODNEW.

(e) Indices of the simple and complex blocks:
  (e_1) for reflection (|IY1(5)| = |ICBNEW|): IY2(3) = IY1(3), IY2(4) = IY1(4), IY2(5) = ICBNEW;
  (e_2) for transmission: IY2(3) = |IY1(5)|, IY2(4) = IY1(7), IY2(5) = ICBNEW.

(f) IY2(6), IY2(7), IY2(8) are undefined.

(g) IY2(9) = IY1(9), IY2(10) = IY1(10), IY2(11) = IY1(11) + 1, IY2(12) = IY1(12).

(h) YY2(I) = YY1(I) for $I = 1, \ldots, 5$.

(i) The real and imaginary parts of the travel time and the coordinates remain unchanged: Y2(I) = Y1(I) for $I = 1, \ldots, 5$.

5.9.2 Metric tensor and velocities

The components G_{ij} and G^{ij} of the metric tensor and the Christoffel symbols Γ^k_{ij} at the point $x^i = \text{Y1}(i+2)$ are the result of the routine METRIC (see Section 2.1).

The parameters of the complex block |IY1(5)| for the incident wave are obtained by invocation of subroutine PARM2. The parameters of the complex block IY1(8) on the other side of the surface IY1(6) are obtained similarly. The velocities VP1, VS1 in the complex block |IY1(5)|, and the velocity v of the incident wave and its derivatives are obtained by invocation of routine VELOC. Similarly, the velocities VP2 and VS2 in the complex block IY1(8) are also obtained by invocation of routine VELOC. In the case of transmission, i.e. if |ICBNEW| = IY1(8), the same invocation yields the velocity $\tilde{v}$ of the transmitted wave, together with its derivatives. In the case of reflection without conversion, i.e. if ICBNEW = IY1(5) then the velocity v with its derivatives is equal to the velocity v of the incident wave with its derivatives. In the case of

reflection with conversion, i.e. if ICBNEW = −IY1(5), the routine VELOC must be called once again to give the velocity $\tilde{v}$ of the reflected wave and its derivatives.

If the velocity $\tilde{v}$ of the reflected/transmitted wave is equal to zero (i.e. an S wave in liquid) then the computation of the ray must be terminated.

5.9.3 *Transformation of the slowness vector and the polarization vectors*

The polarization vectors (basis vectors of the ray-centred coordinate system) of the incident wave are given by

$$H_{i3} = p_i(p_k G^{kl} p_l)^{-1/2},$$

where

$$p_i = \mathrm{Y1}(i+5)$$

is the slowness vector, and by

$$H_{i1} = \mathrm{Y1}(i+8).$$

We define the basis of the local Cartesian coordinate system at the surface IY1(6) specified by $f(x^i) = 0$. The unit normal to the surface is

$$Z_{i3} = f_i(f_k G^{kl} f_l)^{-1/2}.$$

Here we denote $f_i = \partial f/\partial x^i$, $f_{ij} = \partial^2 f/\partial x^i\,\partial x^j$. The cosine of the angle of incidence α $(0 \leq \alpha \leq \pi)$ is

$$\cos\alpha = H_{i3} G^{ij} Z_{j3},$$

and the sine is

$$\sin\alpha = (1 - \cos^2\alpha)^{1/2}.$$

The basis vector in the plane of incidence is

$$Z_{i1} = (H_{i3} - Z_{i3}\cos\alpha)/\sin\alpha,$$

and the basis vector perpendicular to the plane of incidence is

$$Z_{i2} = \varepsilon_{ijk} Z^j{}_3 Z^k{}_1 (\det G_{rs})^{1/2},$$

where $Z^j{}_k = G^{jm} Z_{mk}$ are the contravariant components of the basis vectors, and where $(\det G_{rs})^{1/2}$ is an output parameter of the routine METRIC. In the case of normal incidence, i.e. if $\sin\alpha = 0$, the vectors Z_{i1} and Z_{i2} may be chosen arbitrarily (e.g. $Z_{i1} = H_{i1}$).

The sine of the angle $\tilde{\alpha}$ of reflection/transmission may be evaluated

using Snell's law

$$\sin \tilde{\alpha} = \frac{\tilde{v}}{v} \sin \alpha.$$

The cosine is

$$\cos \tilde{\alpha} = \pm \varepsilon (1 - \sin^2 \tilde{\alpha})^{1/2}, \qquad \varepsilon = \text{sign}\,(\cos \alpha),$$

where the plus sign is taken for transmission (|ICBNEW| = IY1(8)) and the minus sign for reflection (|ICBNEW| = |IY1(5)|).

The revolution angle ψ of the vector Z_{i2} with respect to the polarization vector H_{i2} is determined by

$$\cos \psi = H_{i1} Z^i{}_1 / \cos \alpha, \qquad \sin \psi = -H_{i1} Z^i{}_2.$$

The unit vector perpendicular to the reflected/transmitted ray in the plane of incidence is

$$E_i = Z_{i1} \cos \tilde{\alpha} - Z_{i3} \sin \tilde{\alpha}.$$

The unit vector tangent to the reflected/transmitted ray is

$$\tilde{H}_{i3} = Z_{i1} \sin \tilde{\alpha} + Z_{i3} \cos \tilde{\alpha}.$$

We wish the vector $\tilde{H}_{i2}$ to be rotated with respect to the vector Z_{i2} through the same angle ψ as the vector H_{i2}. Then

$$\text{Y2}(i + 8) = \tilde{H}_{i1} = E_i \cos \psi - Z_{i2} \sin \psi.$$

The slowness vector of the reflected/transmitted ray is

$$\text{Y2}(i + 5) = \tilde{p}_i = \tilde{H}_{i3} / \tilde{v}.$$

5.9.4 *The curvature of the interface and the velocity gradients in the local Cartesian coordinate system*

The second derivatives of the function $f(x^i)$ describing the surface IY1(6) in local Cartesian coordinates divided by the norm of the gradient of $f(x^i)$ are

$$D_{AB} = (f_{ij} - \Gamma^k_{ij} f_k) Z^i{}_A Z^j{}_B (f_r G^{rs} f_s)^{-1/2}.$$

This equation is obtained by transforming the second covariant derivatives of $f(x^i)$ into local Cartesian coordinates.

The velocity gradients in local Cartesian coordinates are

$$V_i = \frac{\partial v}{\partial x^j} Z^j{}_i, \qquad \tilde{V}_i = \frac{\partial \tilde{v}}{\partial x^j} Z^j{}_i.$$

5.9.5 Dynamic ray tracing across a curved interface

First the ray-centred coordinate system is rotated through an angle ψ:

$$Q_{A\beta} = \Psi_{AC}\Pi_{C\beta} = \Psi_{AC}\mathrm{Y1}(7 + C + 4\beta),$$
$$P_{A\beta} = \Psi_{AC}\Pi_{C+2,\beta} = \Psi_{AC}\mathrm{Y1}(9 + C + 4\beta),$$

where

$$\boldsymbol{\Psi} = \begin{bmatrix} \cos\psi & \sin\psi \\ -\sin\psi & \cos\psi \end{bmatrix}.$$

Then the transformation equations are

$$\tilde{Q}_{A\alpha} = \tilde{C}_{AB}C^{-1}_{BC}Q_{C\alpha},$$
$$\tilde{P}_{A\alpha} = \tilde{C}^{-1}_{AB}C_{BC}P_{C\alpha} + \tilde{C}^{-1}_{AB}F_{BC}C^{-1}_{CD}Q_{D\alpha},$$

where

$$\boldsymbol{C} = \begin{bmatrix} \cos\alpha & 0 \\ 0 & 1 \end{bmatrix}, \qquad \tilde{\boldsymbol{C}} = \begin{bmatrix} \cos\tilde{\alpha} & 0 \\ 0 & 1 \end{bmatrix}.$$

The matrix F_{AB} is given by

$$F_{AB} = (v^{-1}\cos\alpha - \tilde{v}^{-1}\cos\tilde{\alpha})D_{AB} + v^{-1}\sin\alpha\,(E_{AB} - \tilde{E}_{AB}),$$

where

$$\boldsymbol{E} = \begin{bmatrix} -V_1v^{-1}(1 + \cos^2\alpha) + V_3v^{-1}\sin\alpha\cos\alpha & -V_2v^{-1} \\ -V_2v^{-1} & 0 \end{bmatrix},$$

$$\tilde{\boldsymbol{E}} = \begin{bmatrix} -\tilde{V}_1\tilde{v}^{-1}(1 + \cos^2\tilde{\alpha}) + \tilde{V}_3\tilde{v}^{-1}\sin\tilde{\alpha}\cos\tilde{\alpha} & -\tilde{V}_2\tilde{v}^{-1} \\ -\tilde{V}_2\tilde{v}^{-1} & 0 \end{bmatrix}.$$

Finally, the ray-centred coordinate system is rotated through an angle $-\psi$

$$\mathrm{Y2}(7 + A + 4\beta) = \tilde{\Pi}_{A\beta} = \Psi_{CA}Q_{C\beta}, \quad \mathrm{Y2}(9 + A + 4\beta) = \tilde{\Pi}_{A+2,\beta} = \Psi_{CA}P_{C\beta}.$$

5.9.6 Transformation of reduced amplitudes

In the case of an incident S wave the ray-centred coordinate system is rotated through an angle ψ

$$\mathrm{Re}\,A_{Ai} = \Psi_{A1}\mathrm{Y1}(28) + \Psi_{A2}\mathrm{Y1}(30), \quad \mathrm{Im}\,A_{Ai} = \Psi_{A1}\mathrm{Y1}(29) + \Psi_{A2}\mathrm{Y1}(31)$$

for $i = 1$ or 3, and, possibly,

$$\mathrm{Re}\,A_{A2} = \Psi_{A1}\mathrm{Y1}(32) + \Psi_{A2}\mathrm{Y1}(34), \quad \mathrm{Im}\,A_{A2} = \Psi_{A1}\mathrm{Y1}(33) + \Psi_{A2}\mathrm{Y1}(35)$$

if there is an S wave at the initial point of the ray. The reduced amplitudes of the incident P wave are not rotated:

$$\mathrm{Re}\, A_{3i} = \mathrm{Y1}(28), \qquad \mathrm{Im}\, A_{3i} = \mathrm{Y1}(29)$$

for $i = 1$ or 3, and, possibly,

$$\mathrm{Re}\, A_{32} = \mathrm{Y1}(30), \qquad \mathrm{Im}\, A_{32} = \mathrm{Y1}(31).$$

Then the above reduced amplitudes are transformed by one of the following equations:

$$\begin{bmatrix} \tilde{A}_{1i} \\ \tilde{A}_{2i} \end{bmatrix} = \left(\frac{\tilde{\rho}\tilde{v}\,|\cos\tilde{\alpha}|}{\rho v\,|\cos\alpha|} \right)^{1/2} \begin{bmatrix} R_{\mathrm{SV}\to\mathrm{SV}} & 0 \\ 0 & R_{\mathrm{SH}\to\mathrm{SH}} \end{bmatrix} \begin{bmatrix} A_{1i} \\ A_{2i} \end{bmatrix},$$

$$\begin{bmatrix} \tilde{A}_{1i} \\ \tilde{A}_{2i} \end{bmatrix} = \left(\frac{\tilde{\rho}\tilde{v}\,|\cos\tilde{\alpha}|}{\rho v\,|\cos\alpha|} \right)^{1/2} \begin{bmatrix} R_{\mathrm{P}\to\mathrm{SV}} \\ 0 \end{bmatrix} A_{3i},$$

$$\tilde{A}_{3i} = \left(\frac{\tilde{\rho}\tilde{v}\,|\cos\tilde{\alpha}|}{\rho v\,|\cos\alpha|} \right)^{1/2} [R_{\mathrm{SV}\to\mathrm{P}} \quad 0] \begin{bmatrix} A_{1i} \\ A_{2i} \end{bmatrix},$$

$$\tilde{A}_{3i} = \left(\frac{\tilde{\rho}\tilde{v}\,|\cos\tilde{\alpha}|}{\rho v\,|\cos\alpha|} \right)^{1/2} R_{\mathrm{P}\to\mathrm{P}} A_{3i},$$

where $i = 1, 2$ for the S wave at the initial point of the ray and $i = 3$ for the P wave at the initial point of the ray.

The reduced amplitudes of generated P waves may be directly stored in the output array Y2,

$$\mathrm{Y2}(28) = \mathrm{Re}\, \tilde{A}_{3i}, \qquad \mathrm{Y2}(29) = \mathrm{Im}\, \tilde{A}_{3i}$$

for $i = 1$ or 3, and, for an S wave at the initial point of the ray,

$$\mathrm{Y2}(30) = \mathrm{Re}\, \tilde{A}_{32}, \qquad Y2(31) = \mathrm{Im}\, \tilde{A}_{32}.$$

For S waves the ray-centred coordinate system is rotated through an angle $-\psi$,

$$\mathrm{Y2}(26 + 2A) = \Psi_{BA}\, \mathrm{Re}\, \tilde{A}_{Bi}, \qquad \mathrm{Y2}(27 + 2A) = \Psi_{BA}\, \mathrm{Im}\, \tilde{A}_{Bi}$$

for $i = 1$ or 3, and, for an S wave at the initial point of the ray,

$$\mathrm{Y2}(30 + 2A) = \Psi_{BA}\, \mathrm{Re}\, \tilde{A}_{B2}, \qquad \mathrm{Y2}(31 + 2A) = \Psi_{BA}\, \mathrm{Im}\, \tilde{A}_{B2}.$$

5.9.7 The reflection/transmission coefficients

The R/T coefficients are given by the following expressions:

Reflection coefficients

$$\begin{aligned}
R_{SV\to SV} &= D^{-1}[q^2p^2P_1P_2P_3P_4 + \rho_1\rho_2(\alpha_1\beta_2P_2P_3 - \beta_1\alpha_2P_1P_4) \\
&\quad - \alpha_1\beta_1P_3P_4Y^2 + \alpha_2\beta_2P_1P_2X^2 - \alpha_1\alpha_2\beta_1\beta_2p^2Z^2], \\
R_{P\to P} &= D^{-1}[q^2p^2P_1P_2P_3P_4 + \rho_1\rho_2(\beta_1\alpha_2P_1P_4 - \alpha_1\beta_2P_2P_3) \\
&\quad - \alpha_1\beta_1P_3P_4Y^2 + \alpha_2\beta_2P_1P_2X^2 - \alpha_1\alpha_2\beta_1\beta_2p^2Z^2], \\
R_{SV\to P} &= -2\varepsilon\beta_1pP_2D^{-1}(qP_3P_4Y + \alpha_2\beta_2XZ), \\
R_{P\to SV} &= 2\varepsilon\alpha_1pP_1D^{-1}(qP_3P_4Y + \alpha_2\beta_2XZ), \\
R_{SH\to SH} &= \bar{D}^{-1}(\rho_1\beta_1P_2 - \rho_2\beta_2P_4);
\end{aligned}$$

Transmission coefficients

$$\begin{aligned}
R_{SV\to SV} &= 2\beta_1\rho_1P_2D^{-1}(\alpha_1P_3Y + \alpha_2P_1X), \\
R_{P\to P} &= 2\alpha_1\rho_1P_1D^{-1}(\beta_2P_2X + \beta_1P_4Y), \\
R_{SV\to P} &= 2\varepsilon\beta_1\rho_1pP_2D^{-1}(qP_1P_4 - \alpha_1\beta_2Z), \\
R_{P\to SV} &= -2\varepsilon\alpha_1\rho_1pP_1D^{-1}(qP_2P_3 - \beta_1\alpha_2Z), \\
R_{SH\to SH} &= 2\rho_1\beta_1P_2\bar{D}^{-1}.
\end{aligned}$$

Here

$$\begin{aligned}
D &= q^2p^2P_1P_2P_3P_4 + \rho_1\rho_2(\beta_1\alpha_2P_1P_4 + \alpha_1\beta_2P_2P_3) \\
&\quad + \alpha_1\beta_1P_3P_4Y^2 + \alpha_2\beta_2P_1P_2X^2 + \alpha_1\alpha_2\beta_1\beta_2p^2Z^2, \\
\bar{D} &= \rho_1\beta_1P_2 + \rho_2\beta_2P_4, \\
q &= 2(\rho_2\beta_2^2 - \rho_1\beta_1^2), \quad X = \rho_2 - qp^2, \quad Y = \rho_1 + qp^2, \quad Z = \rho_2 - \rho_1 - qp^2, \\
P_1 &= (1 - \alpha_1^2p^2)^{1/2}, \quad P_2 = (1 - \beta_1^2p^2)^{1/2}, \\
P_3 &= (1 - \alpha_2^2p^2)^{1/2}, \quad P_4 = (1 - \beta_2^2p^2)^{1/2}.
\end{aligned}$$

The square roots P_κ are positive imaginary for negative argument, e.g. $P_3 = \mathrm{i}(\alpha_2^2p^2 - 1)^{1/2}$ for $p > 1/\alpha_2$. The quantity p is the ray parameter, $p = \sin\alpha/v$, where α is the angle of incidence, $0 \leq \alpha \leq \pi$ (see Section 5.9.3), and v is the velocity of the incident wave at the point of incidence. The quantities $\alpha_1 = \mathrm{VP1}$, $\beta_1 = \mathrm{VS1}$ and ρ_1 correspond to the point of incidence at that side of the interface containing the incident wave; $\alpha_2 = \mathrm{VP2}$, $\beta_2 = \mathrm{VS2}$ and ρ_2 correspond to the other side of the interface at the same point. The quantity ε is given by the relation $\varepsilon = \mathrm{sign}\,(\cos\alpha)$ (see Section 5.9.3). For further details see Červený (1985a).

For a liquid–liquid interface we have

$$R_{P\to P}=\frac{\rho_2\alpha_2P_1-\rho_1\alpha_1P_3}{\rho_2\alpha_2P_1+\rho_1\alpha_1P_3}$$

for reflection, and

$$R_{P\to P}=\frac{2\rho_1\alpha_1P_1}{\rho_2\alpha_2P_1+\rho_1\alpha_1P_3}$$

for transmission.

For reflections from the Earth's surface we put $\alpha_2=\beta_2=\rho_2=0$ in the above expressions.

6 INITIAL POINTS OF RAYS

Let us consider a two-parameter system of rays of a specified elementary wave. A ray of the elementary wave is specified by its two parameters γ^1 and γ^2. The computed rays may start from a single initial point common to all rays, from an initial surface along which an initial travel time is defined, from a curve along which an initial travel time is defined, etc.

6.1 Important quantities at the initial point of the ray

At the initial point of the ray, we are interested in particular in the quantities ICB1 and YL(1), . . . , YL(6), defined in Section 5.5.4 and describing the local properties of the model, and in the following quantities describing the properties of the rays and of the travel-time field:

YI(1)	initial travel time;
YI(2)	initial imaginary part of the complex travel time;
YI(3), . . . , YI(5)	coordinates of the initial point of the ray;
YI(6), . . . , YI(8)	covariant components of the initial slowness vector;
YI(9), . . . , YI(11)	covariant components of the first basis vector of the ray-centred coordinate system at the initial point of the ray (perpendicular to the slowness vector YI(6), . . . , YI(8));

$$\begin{bmatrix} \text{YI(12)} & \text{YI(16)} \\ \text{YI(13)} & \text{YI(17)} \\ \text{YI(14)} & \text{YI(18)} \\ \text{YI(15)} & \text{YI(19)} \end{bmatrix}$$

the elements of the matrix $\boldsymbol{Q}^{\mathrm{R}}$ of geometrical spreading, and the matrix $\boldsymbol{P}^{\mathrm{R}}$, at the initial point of the ray, see (5.13);

$$= \begin{bmatrix} Q_{11}^{\mathrm{INIT}} & Q_{12}^{\mathrm{INIT}} \\ Q_{21}^{\mathrm{INIT}} & Q_{22}^{\mathrm{INIT}} \\ P_{11}^{\mathrm{INIT}} & P_{12}^{\mathrm{INIT}} \\ P_{21}^{\mathrm{INIT}} & P_{22}^{\mathrm{INIT}} \end{bmatrix},$$

$\mathrm{YI}(20) = \tilde{\gamma}^1$, $\mathrm{YI}(21) = \tilde{\gamma}^2$ take-off parameters of the computed ray.

In addition to the above quantities describing the properties defined for a single ray, there are also quantities describing the properties of the discrete system of computed rays in the vicinity of the computed ray. Of these quantities, we are interested in particular in the following:

YI(22) area Γ of element $\delta\Gamma$ of the ray-parameter surface, corresponding to the ray,

$$\Gamma = \int_{\delta\Gamma} \mathrm{d}\gamma^1 \, \mathrm{d}\gamma^2; \tag{6.1}$$

YI(23), YI(24), YI(25) components Γ_{11}, Γ_{12}, Γ_{22} of the symmetric matrix Γ_{KL} inverse to the specific moment

$$\Gamma^{IJ} = \Gamma^{-1} \int_{\delta\Gamma} (\tilde{\gamma}^I - \gamma^I)(\tilde{\gamma}^J - \gamma^J) \, \mathrm{d}\gamma^1 \, \mathrm{d}\gamma^2 \tag{6.2}$$

of the element $\delta\Gamma$ of the ray-parameter surface, evaluated with respect to the ray. Here γ^I are the ray parameters.

The quantities ICB1, YL(1), . . . , YL(6) and YI(1), . . . , YI(21) corresponding to the initial point of the ray, together with the quantities YI(22), . . . , YI(25), are required in processing the results of complete ray tracing; they must be stored in some file. The quantities YI(22), . . . , YI(25) are not generally known during complete ray tracing; they can be determined after it. Thus they cannot be stored when the results of complete ray tracing are stored, but must be stored after the complete tracing of the ray has been finished. For these reasons, the quantities YI(22), . . . , YI(25) should be stored in another file than that where the results of the complete ray tracing are stored. It seems reasonable to store all the quantities ICB1, YL(1), . . . , YL(6) and

YI(1), . . . , YI(25) corresponding to the initial points of rays in a separate file.

The index ISB1 of the simple block containing the initial point of the ray, and abovementioned quantities ICB1, YL(1), . . . , YL(6), YI(1), . . . , YI(21) defined at the initial point of the ray, may be necessary or useful during the complete tracing of the ray. For this reason, they should be stored in a common block.

6.2 Initial values for complete ray tracing

The initial values of the basic quantities Y(1), . . . , Y(NY), where NY = 27 + NAMPL, computed along a ray and defined in Section 5.2.1, are

$$Y(I) = YI(I) \quad \text{for } I = 1, \ldots, 11;$$

$$\begin{bmatrix} Y(12) & Y(16) & Y(20) & Y(24) \\ Y(13) & Y(17) & Y(21) & Y(25) \\ Y(14) & Y(18) & Y(22) & Y(26) \\ Y(15) & Y(19) & Y(23) & Y(27) \end{bmatrix} = \begin{bmatrix} 1 & 0 & 0 & 0 \\ 0 & 1 & 0 & 0 \\ 0 & 0 & 1 & 0 \\ 0 & 0 & 0 & 1 \end{bmatrix};$$

and

(a) for a P wave at the initial point of the ray

$$NAMPL = 2,$$
$$Y(28) = 1, \qquad Y(29) = 0;$$

(b) for an S wave at the initial point of the ray

$$NAMPL = 8,$$
$$Y(28) = 1, \qquad Y(29) = 0,$$
$$Y(30) = 0, \qquad Y(31) = 0,$$
$$Y(32) = 0, \qquad Y(33) = 0,$$
$$Y(34) = 1, \qquad Y(35) = 0.$$

The initial values of the auxiliary quantities defined in Section 5.2.2 are

$$YY(1) = 0;$$
$$YY(2) = UEB,$$

which is the value specified in the input data (see Section 5.6);

$$YY(3) = 0, \qquad YY(4) = 0, \qquad YY(5) = 0;$$
$$IY(1) = 27 + NAMPL,$$

where NAMPL is given above;

$$\text{IY(2)} = 0, \qquad \text{IY(3)} = 0;$$
$$\text{IY(4)} = \text{ISB1},$$

where ISB1 is the index of the simple block in which the initial point of the ray is situated;

$$\text{IY(5)} = \text{ICB1},$$

where ICB1 is the index of the complex block in which the initial point of the ray is situated, together with sign + for a P wave and − for an S wave;

$$\text{IY(6)} \quad \text{undefined} \quad (\text{e.g. IY(6)} = 0);$$
$$\text{IY(7)} \quad \text{undefined} \quad (\text{e.g. IY(7)} = 0);$$
$$\text{IY(8)} \quad \text{undefined} \quad (\text{e.g. IY(8)} = 0);$$
$$\text{IY(9)} = 0, \qquad \text{IY(10)} = 0, \qquad \text{IY(11)} = 0, \qquad \text{IY(12)} = 0.$$

7 APPLICATIONS AND PROCESSING OF THE RESULTS OF COMPLETE RAY TRACING

Using the complete ray-tracing procedure described here, we determine and store various quantities of great seismological importance along the ray and at intersections of the ray with some selected surfaces. Moreover, additional routines can be used to modify and/or considerably generalize the initial conditions used in the procedure and to process the results. In this way, the complete ray-tracing procedure can be used as a basic procedure in many program packages dealing with high-frequency seismic body waves propagating in complex 3D laterally varying layered and block structures. In this section we shall briefly describe several such possibilities. We believe that complete ray tracing will find many other important seismological applications, in addition to those listed in this section, in the near future.

We denote here the computed ray by Ω, the initial point of the ray by 0_0, and another point of the ray Ω by 0_s. We shall also consider a point S situated close to the point 0_s, and a point 0 close to 0_0 (see Fig. 7). The general coordinates of these points are denoted by $x^i(0_0)$, $x^i(0_s)$, $x^i(S)$ and $x^i(0)$ respectively. The coordinates of the initial point 0_0 are specified in the initial conditions, see YI(3), . . . , YI(5) in Section 6.1, and the coordinates of the point 0_s are obtained by the complete ray tracing, see Y(3), . . . , Y(5) in Section 5.2.1.

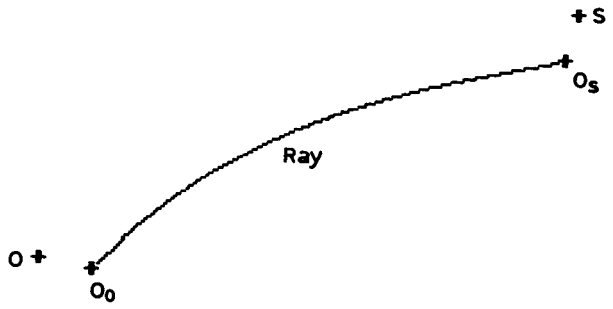

Fig. 7

7.1 Travel time. Imaginary travel time

We denote the initial travel time by $\tau_0 = \tau(0_0)$, and the initial imaginary travel time (i.e. the imaginary part of the complex-valued travel time) by $\tau^{IM}(0_0)$. They are specified by YI(1) and YI(2) in the initial conditions (see Section 6.1). By complete ray tracing we obtain $\tau(0_s)$, the arrival time of the wave under consideration at 0_s, and $\tau^{IM}(0_s)$, the imaginary part of the complex-valued arrival time, see Y(1) and Y(2) in Section 5.2.1. We introduce the travel time $\tau(0_s, 0_0)$ and the imaginary travel time $\tau^{IM}(0_s, 0_0)$ from 0_0 to 0_s along Ω by the relations

$$\left.\begin{aligned} &\tau(0_s, 0_0) = \tau(0_s) - \tau(0_0), \\ &\tau^{IM}(0_s, 0_0) = \tfrac{1}{2}t^*(0_s, 0_0) = \tau^{IM}(0_s) - \tau^{IM}(0_0). \end{aligned}\right\} \tag{7.1}$$

Instead of $\tau^{IM}(0_s, 0_0)$, we shall also use $\frac{1}{2}t^*(0_s, 0_0)$, and call t^* the "t-star". The importance of the travel time $\tau(0_s, 0_0)$ is obvious; the quantity t^* plays an important role in the evaluation of the amplitudes of waves propagating in dissipative media (see Section 7.18).

7.2 Slowness vector. First partial derivatives of the travel-time field

At the initial point 0_0 the covariant components of the slowness vector $p_i(0_0)$ are given by YI(6), . . . , YI(8) (see Section 6.1). At 0_s they are obtained by complete ray tracing, see Y(6), . . . , Y(8) in Section 5.2.1. In both cases they represent the first partial derivatives of the travel-time field with respect to the general coordinates x^i:

$$p_i(0_0) = \left[\frac{\partial\tau(P)}{\partial x^i}\right]_{P=0_0}, \qquad p_i(0_s) = \left[\frac{\partial\tau(P)}{\partial x^i}\right]_{P=0_s}. \tag{7.2}$$

Thus $p_i(0_0)$ can be used in the hypocentre location procedures, as $-p_i(0_0)$ represent the partial derivatives of the travel time $\tau(0_s, 0_0)$ with respect to the coordinates of the source 0_0. Equations (7.2) can be also used in the calculation of the paraxial travel times (see Section 7.10).

From the covariant components $p_i(0_0)$ and $p_i(0_s)$, we can easily obtain the contravariant components using the relations

$$p^i(0_0) = G^{ik}(0_0)p_k(0_0), \qquad p^i(0_s) = G^{ik}(0_s)p_k(0_s). \tag{7.3}$$

7.3 Vector basis of the ray-centred coordinate system

The basis vectors of the ray-centred coordinate system $\boldsymbol{e}_1$, $\boldsymbol{e}_2$, $\boldsymbol{e}_3 = \boldsymbol{t}$ (also called the polarization vectors) are easily evaluated from the quantities obtained by complete ray tracing.

The unit vector $\boldsymbol{t}$ is tangent to the ray, so it is immediately obtained from the slowness vector:

$$\left.\begin{aligned} t_i(0_0) &= v(0_0)p_i(0_0), \qquad t_i(0_s) = v(0_s)p_i(0_s), \\ t^i(0_0) &= v(0_0)p^i(0_0), \qquad t^i(0_s) = v(0_s)p^i(0_s). \end{aligned}\right\} \tag{7.4}$$

The triplet $\boldsymbol{e}_1$, $\boldsymbol{e}_2$, $\boldsymbol{e}_3 = \boldsymbol{t}$ is mutually perpendicular at any point of the ray. The initial unit vectors $\boldsymbol{e}_1(0_0)$ and $\boldsymbol{e}_2(0_0)$ satisfying this property may be chosen arbitrarily.

We denote by $H^{\mathrm{U}}_{ij}(0_0)$ the ith covariant component of the initial polarization vector $\boldsymbol{e}_j(0_0)$, and, similarly, by $H^{\mathrm{U}}_{ij}(0_s)$ the ith covariant component of the polarization vector $\boldsymbol{e}_j(0_s)$. We assume that the vector H^{U}_{i3} is perpendicular to the wavefront. In this section we shall call the following choice of initial polarization vectors the *intrinsic choice*:

$$H^{\mathrm{U}}_{ij}(0_0) = H_{ij}(0_0), \tag{7.5}$$

where

$$\left.\begin{aligned} H_{i3}(0_0) &= t_i(0_0), \\ H_{i1}(0_0) &= \mathrm{YI}(i+8), \\ H_{i2}(0_0) &= \varepsilon_{ijk}G^{jm}(0_0)H_{m3}(0_0)G^{kn}(0_0)H_{n1}(0_0)[\det G^{rs}(0_0)]^{-1/2}. \end{aligned}\right\} \tag{7.6}$$

The intrinsic choice of polarization vectors is implicitly used in the procedure of complete ray tracing proposed here. Any general choice $H^{\mathrm{U}}_{ij}(0_0)$ of the initial polarization vectors $\boldsymbol{e}_j(0_0)$ will be called here the *user's choice*. Of course, the matrix $H^{\mathrm{U}}_{ij}(0_0)$ must be specified by the user; we assume here that it is known.

At the point 0_s, the covariant components $H^{\mathrm{U}}_{ij}(0_s)$ of the polarization

vectors $\boldsymbol{e}_j(0_s)$ are given by the relation

$$H_{ij}^{\mathrm{U}}(0_s) = H_{ik}(0_s)H_{mk}(0_0)G^{mn}(0_0)H_{nj}^{\mathrm{U}}(0_0), \tag{7.7}$$

where

$$\left.\begin{aligned} &H_{i3}(0_s) = t_i(0_s), \\ &H_{i1}(0_s) = \mathrm{Y}(i+8), \\ &H_{i2}(0_s) = \varepsilon_{ijk}G^{jm}(0_s)H_{m3}(0_s)G^{kn}(0_s)H_{n1}(0_s)[\det G^{rs}(0_s)]^{-1/2}. \end{aligned}\right\} \tag{7.8}$$

Let us conclude that for any user's choice of the initial polarization vectors at 0_0 we can evaluate the polarization vectors at 0_s using $\mathrm{Y}(6), \ldots, \mathrm{Y}(11)$ and the above equations.

For the intrinsic choice (7.5) of initial polarization vectors, (7.7) simplifies to

$$H_{ij}^{\mathrm{U}}(0_s) = H_{ij}(0_s). \tag{7.9}$$

Note that the quantities H_{ij}^{U} represent the elements of the 3×3 transformation matrix from the user's ray-centred to the general coordinate system. Similarly, H_{ij} represent the elements of the 3×3 transformation matrix from the intrinsic ray-centred to the general coordinate system.

The 3×3 transformation matrix $\hat{\boldsymbol{H}}^{\mathrm{UI}}$ from the intrinsic ray-centred to the user's ray-centred coordinate system,

$$H_{jk}^{\mathrm{UI}} = H_{mj}^{\mathrm{U}}(0_0)G^{mn}(0_0)H_{nk}(0_0), \tag{7.10}$$

is constant along the ray.

7.4 Ray propagator matrix

The elements of the 4×4 propagator matrix $\boldsymbol{\Pi}(0_s, 0_0)$ at 0_s are stored in $\mathrm{Y}(12), \ldots, \mathrm{Y}(27)$ (see Section 5.2.1). Remember that $\boldsymbol{\Pi}(0_0, 0_0) = \boldsymbol{I}$, where $\boldsymbol{I}$ is the 4×4 identity matrix (see Section 6.2). The ray propagator matrix is expressed in the intrinsic ray-centred coordinates.

We introduce the 2×2 real-valued matrices $\boldsymbol{Q}_1(0_s, 0_0)$, $\boldsymbol{Q}_2(0_s, 0_0)$, $\boldsymbol{P}_1(0_s, 0_0)$ and $\boldsymbol{P}_2(0_s, 0_0)$ by the relation

$$\boldsymbol{\Pi}(0_s, 0_0) = \begin{bmatrix} \boldsymbol{Q}_1(0_s, 0_0) & \boldsymbol{Q}_2(0_s, 0_0) \\ \boldsymbol{P}_1(0_s, 0_0) & \boldsymbol{P}_2(0_s, 0_0) \end{bmatrix}. \tag{7.11}$$

Here $\boldsymbol{Q}_1(0_s, 0_0)$ and $\boldsymbol{P}_1(0_s, 0_0)$ are the matrix solutions of the dynamic ray-tracing system (5.15), with the telescopic (plane-wavefront) initial

conditions at 0_0. Similarly, $\boldsymbol{Q}_2(0_s, 0_0)$ and $\boldsymbol{P}_2(0_s, 0_0)$ correspond to the point-source initial conditions at 0_0.

Note that the inverse of the ray propagator matrix is given by

$$\boldsymbol{\Pi}(0_0, 0_s) = \boldsymbol{\Pi}^{-1}(0_s, 0_0) = \begin{bmatrix} \boldsymbol{P}_2^{\mathrm{T}}(0_s, 0_0) & -\boldsymbol{Q}_2^{\mathrm{T}}(0_s, 0_0) \\ -\boldsymbol{P}_1^{\mathrm{T}}(0_s, 0_0) & \boldsymbol{Q}_1^{\mathrm{T}}(0_s, 0_0) \end{bmatrix}, \tag{7.12}$$

which follows from (5.11). Thus, using the results of complete ray tracing from 0_0 to 0_s, we can also determine the inverse ray propagator matrix from 0_s to 0_0.

7.5 Matrix of geometrical spreading Q

The 2×2 matrix of geometrical spreading

$$Q_{AB} = \left[\frac{\partial q^A}{\partial \gamma^B}\right]_{q^1=q^2=0} \tag{7.13}$$

represents the transformation matrix from ray coordinates (γ^1, γ^2) to the user's ray-centred coordinates (q^1, q^2). The general relation for the matrix of geometrical spreading at the point 0_s is

$$\boldsymbol{Q}(0_s) = \boldsymbol{H}^{\mathrm{UI}}\{\boldsymbol{Q}_1(0_s, 0_0)(\boldsymbol{H}^{\mathrm{UI}})^{\mathrm{T}}\boldsymbol{Q}(0_0) + \boldsymbol{Q}_2(0_s, 0_0)(\boldsymbol{H}^{\mathrm{UI}})^{\mathrm{T}}\boldsymbol{P}(0_0)\}. \tag{7.14}$$

The transformation matrix $\boldsymbol{P}$ from the ray coordinates to the user's ray-centred components of the slowness vector is defined in Section 7.6.

Equation (7.14) is valid for any system of rays containing the ray Ω and for any parametrization of the rays, not only for the initial conditions and the ray parametrization specified before the complete ray tracing of the ray Ω (see Section 6). For this reason, we use here the notation $\boldsymbol{Q}$ instead of $\boldsymbol{Q}^{\mathrm{R}}$, see (5.13). Note that the change from the parameters γ^A to the parameters $\bar{\gamma}^A$ (for a fixed system of rays) represents the multiplication of both left- and right-hand sides of (7.14) by a constant 2×2 matrix

$$C_{AB} = \frac{\partial \gamma^A}{\partial \bar{\gamma}^B}. \tag{7.15}$$

Considering the system of rays and its parametrization specified for the complete tracing of the ray Ω (see Section 6), we can evaluate the matrix of geometrical spreading at the initial point of the ray in the user's ray-centred coordinates as

$$\boldsymbol{Q}(0_0) = \boldsymbol{H}^{\mathrm{UI}}\boldsymbol{Q}^{\mathrm{INIT}}, \tag{7.16}$$

where the components of the 2×2 matrix $\boldsymbol{Q}^{\mathrm{INIT}}$ are stored in YI(12), YI(13), YI(16), YI(17). Similarly,

$$\boldsymbol{P}(0_0) = \boldsymbol{H}^{\mathrm{UI}}\boldsymbol{P}^{\mathrm{INIT}}, \tag{7.17}$$

where $\boldsymbol{P}^{\mathrm{INIT}}$ is stored in YI(14), YI(15), YI(18), YI(19) (see Section 6.1). Then (7.14) reads

$$\boldsymbol{Q}(0_s) = \boldsymbol{H}^{\mathrm{UI}}\{\boldsymbol{Q}_1(0_s, 0_0)\boldsymbol{Q}^{\mathrm{INIT}} + \boldsymbol{Q}_2(0_s, 0_0)\boldsymbol{P}^{\mathrm{INIT}}\}. \tag{7.18}$$

7.6 Transformation matrix $\boldsymbol{P}$

The 2×2 matrix $\boldsymbol{P}$ with components

$$P_{AB} = \left[\frac{\partial p_A^{(q)}}{\partial \gamma^B}\right]_{q^1, q^2 = 0}$$

represents the transformation matrix from ray coordinates (γ^1, γ^2) to the user's ray-centred components $p_1^{(q)} = \partial\tau/\partial q^1$, $p_2^{(q)} = \partial\tau/\partial q^2$ of the slowness vector. The general relation for the matrix $\boldsymbol{P}$ is

$$\boldsymbol{P}(0_s) = \boldsymbol{H}^{\mathrm{UI}}\{\boldsymbol{P}_1(0_s, 0_0)(\boldsymbol{H}^{\mathrm{UI}})^{\mathrm{T}}\boldsymbol{Q}(0_0) + \boldsymbol{P}_2(0_s, 0_0)(\boldsymbol{H}^{\mathrm{UI}})^{\mathrm{T}}\boldsymbol{P}(0_0)\}. \tag{7.19}$$

The discussion of this equation and the meaning of the individual quantities is similar to those in Section 7.5.

For the system of rays and its parametrization specified for complete ray tracing along the ray Ω, $\boldsymbol{Q}(0_0) = \boldsymbol{H}^{\mathrm{UI}}\boldsymbol{Q}^{\mathrm{INIT}}$, $\boldsymbol{P}(0_0) = \boldsymbol{H}^{\mathrm{UI}}\boldsymbol{P}^{\mathrm{INIT}}$ (see Section 7.5), (7.19) yields

$$\boldsymbol{P}(0_s) = \boldsymbol{H}^{\mathrm{UI}}\{\boldsymbol{P}_1(0_s, 0_0)\boldsymbol{Q}^{\mathrm{INIT}} + \boldsymbol{P}_2(0_s, 0_0)\boldsymbol{P}^{\mathrm{INIT}}\}. \tag{7.20}$$

7.7 Geometrical spreading

By the geometrical spreading $J(0_s)$, we understand here the quantity

$$J(0_s) = |\det \boldsymbol{Q}(0_s)|. \tag{7.21a}$$

The geometrical spreading can be evaluated if the matrix of geometrical spreading $\boldsymbol{Q}$ is known. The geometrical spreading does not depend on the initial orientation of the polarization vectors $\boldsymbol{e}_1(0_0)$ and $\boldsymbol{e}_2(0_0)$.

For a point source at 0_0, (7.21a) yields

$$J(0_s) = |\det \boldsymbol{Q}_2(0_s, 0_0)|\,|\det \boldsymbol{P}(0_0)|. \tag{7.21b}$$

The geometrical spreading is of great importance in the evaluation of

ray amplitudes: the ray amplitudes are inversely proportional to the square root of geometrical spreading.

7.8 Matrix of second derivatives of the travel-time field

The elements of the 2×2 matrix $\boldsymbol{M}$ of the second derivatives of the travel-time field with respect to the user's ray-centred coordinates (q^1, q^2), $M_{JK} = [\partial^2 \tau / \partial q^J \, \partial q^K]_{q^1=q^2=0}$, can be evaluated by $\boldsymbol{M} = \boldsymbol{P}\boldsymbol{Q}^{-1}$ both at the initial point 0_0 and at 0_s. Using (7.14) and (7.19), we obtain the continuation formula for $\boldsymbol{M}$ as

$$\boldsymbol{M}(0_s) = \boldsymbol{H}^{\mathrm{UI}}\{\boldsymbol{P}_1(0_s, 0_0) + \boldsymbol{P}_2(0_s, 0_0)(\boldsymbol{H}^{\mathrm{UI}})^{\mathrm{T}}\boldsymbol{M}(0_0)\boldsymbol{H}^{\mathrm{UI}}\} \times \{\boldsymbol{Q}_1(0_s, 0_0) + \boldsymbol{Q}_2(0_s, 0_0)(\boldsymbol{H}^{\mathrm{UI}})^{\mathrm{T}}\boldsymbol{M}(0_0)\boldsymbol{H}^{\mathrm{UI}}\}^{-1}(\boldsymbol{H}^{\mathrm{UI}})^{\mathrm{T}}. \quad (7.22)$$

Let us now consider a local Cartesian coordinate system (y^1, y^2, y^3) at 0_s, with $y^1 = q^1$, $y^2 = q^2$ and with y^3 being the length coordinate measured along the tangent to the ray Ω at 0_s. Then the 3×3 matrix $\hat{\boldsymbol{M}}(0_s)$, with elements $M_{ij} = [\partial^2 \tau / \partial y^i \, \partial y^j]_{0_s}$, is given by

$$\hat{\boldsymbol{M}}(0_s) = \begin{bmatrix} M_{11}(0_s) & M_{12}(0_s) & -V_1 v^{-2} \\ M_{12}(0_s) & M_{22}(0_s) & -V_2 v^{-2} \\ -V_1 v^{-2} & -V_2 v^{-2} & -V_3 v^{-2} \end{bmatrix}, \quad (7.23)$$

where

$$V_j = \frac{\partial v}{\partial x^m} G^{mn} H_{nj} \quad (7.24)$$

is the velocity gradient in the local Cartesian coordinates y^j at 0_s.

Finally, we introduce the 3×3 matrix $\hat{\boldsymbol{N}}(0_s)$, with elements $N_{ij}(0_s) = [\partial^2 \tau / \partial x^i \, \partial x^j]_{0_s}$ given by

$$N_{jk}(0_s) = H_{jm}(0_s) H_{kn}(0_s) M_{mn}(0_s) + \Gamma^s_{jk}(0_s) p_s(0_s). \quad (7.25)$$

7.9 Curvature of the wavefront

The 2×2 matrix of the curvature of the wavefront $\boldsymbol{K}$ in the user's ray-centred coordinate system can be simply evaluated from the 2×2 matrix $\boldsymbol{M}$ using the relation

$$\boldsymbol{K} = v\boldsymbol{M} = v\boldsymbol{P}\boldsymbol{Q}^{-1}. \quad (7.26)$$

Thus we have

$$\boldsymbol{K}(0_0) = v(0_0)\boldsymbol{M}(0_0), \qquad \boldsymbol{K}(0_s) = v(0_s)\boldsymbol{M}(0_s).$$

Similarly, the 2×2 matrix of the radii of curvature $\boldsymbol{R}$ is given by

$$\boldsymbol{R} = \boldsymbol{K}^{-1} = v^{-1}\boldsymbol{M}^{-1} = v^{-1}\boldsymbol{Q}\boldsymbol{P}^{-1}. \tag{7.27}$$

Using $\boldsymbol{K}$ (or $\boldsymbol{R}$), we can determine the main geometrical characteristics of the wavefront (the principal curvatures, the principal directions, the wavefront ellipse or the wavefront hyperbola, etc.). For details see Červený and Pšenčík (1983b).

7.10 Paraxial travel times

By the paraxial travel times, we understand the travel times in the vicinity of the central ray Ω.

Let us consider a single initial point at 0_0 and denote

$$x^k(S, 0_s) = x^k(S) - x^k(0_s), \qquad x^k(0, 0_0) = x^k(0) - x^k(0_0). \tag{7.28}$$

Then the results of complete ray tracing from 0_0 to 0_s can be used to find not only the travel time from 0_0 to 0_s, but also approximate expressions for the travel time from 0_0 to S or even for the travel time from 0 to S if S is close to 0_s and 0 is close to 0_0:

$$\tau(S, 0_0) = \tau(0_s, 0_0) + p_k(0_s)x^k(S, 0_s) + \tfrac{1}{2}x^m(S, 0_s)x^n(S, 0_s)N_{mn}(0_s, 0_0). \tag{7.29}$$

Similarly, we obtain (see Červený *et al.*, 1984)

$$\begin{aligned}\tau(S, 0) = \tau(0_s, 0_0) &+ x^k(S, 0_s)p_k(0_s) - x^k(0, 0_0)p_k(0_0) \\ &+ \tfrac{1}{2}x^m(S, 0_s)N_{mn}(0_s, 0_0)x^n(S, 0_s) \\ &- \tfrac{1}{2}x^m(0, 0_0)N_{mn}(0_0, 0_s)x^n(0, 0_0) \\ &- x^j(0, 0_0)H_{jJ}(0_0)[Q_2^{-1}(0_s, 0_0)]_{JK}H_{kK}(0_s)x^k(S, 0_s).\end{aligned} \tag{7.30}$$

In (7.29) and (7.30) $N_{mn}(0_s, 0_0)$ (respectively $N_{mn}(0_0, 0_s)$) are elements of the 3×3 matrix $\hat{\boldsymbol{N}}(0_s, 0_0)$ (respectively $\hat{\boldsymbol{N}}(0_0, 0_s)$) of the second derivatives of the travel time field with respect to the general coordinates x^i at the point 0_s (respectively 0_0) due to a point source at 0_0 (respectively 0_s). They are given by (7.25) and (7.23), where M_{JK} are replaced by

$$\boldsymbol{M}(0_s, 0_0) = \boldsymbol{P}_2(0_s, 0_0)(\boldsymbol{Q}_2(0_s, 0_0))^{-1} \tag{7.31a}$$

(respectively

$$\boldsymbol{M}(0_0, 0_s) = -(\boldsymbol{Q}_2(0_s, 0_0))^{-1}\boldsymbol{Q}_1(0_s, 0_0). \tag{7.31b})$$

Equations (7.29) and (7.30) are, of course, only approximate; they are valid for small $x^i(S, 0_s)$ and $x^i(0, 0_0)$.

7.11 Paraxial rays

Paraxial rays are rays situated *close to the central ray* Ω. If the ray propagator matrix is known along Ω then the paraxial rays can be approximately evaluated analytically.

Let us first consider the simplest problem of *initial-value paraxial ray tracing*. We assume that the initial point 0 of the paraxial ray is situated in a plane perpendicular to Ω at 0_0 and denote its user's ray-centred coordinates by $(q^1(0), q^2(0))$. Similarly, we assume that the point S is situated in the plane perpendicular to Ω at 0_s and denote its user's ray-centred coordinates by $(q^1(S), q^2(S))$. We denote the user's ray-centred components of the slowness vector at 0 by $p_1^{(q)}(0)$ and $p_2^{(q)}(0)$, and those at S by $p_1^{(q)}(S)$ and $p_2^{(q)}(S)$. We also denote

$$\left.\begin{aligned} \boldsymbol{W}(0_0) &= [q^1(0) \quad q^2(0) \quad p_1^{(q)}(0) \quad p_2^{(q)}(0)]^{\mathrm{T}}, \\ \boldsymbol{W}(0_s) &= [q^1(S) \quad q^2(S) \quad p_1^{(q)}(S) \quad p_2^{(q)}(S)]^{\mathrm{T}}. \end{aligned}\right\} \tag{7.32}$$

Then the dynamic ray-tracing system yields the following analytical solution for the initial conditions given by $\boldsymbol{W}(0_0)$:

$$\boldsymbol{W}(0_s) = \boldsymbol{U\Pi}(0_s, 0_0)\boldsymbol{U}^{\mathrm{T}}\boldsymbol{W}(0_0), \tag{7.33}$$

where $\boldsymbol{U}$ is the 4×4 matrix given by

$$\boldsymbol{U} = \begin{pmatrix} \boldsymbol{H}^{\mathrm{UI}} & \boldsymbol{0} \\ \boldsymbol{0} & \boldsymbol{H}^{\mathrm{UI}} \end{pmatrix}. \tag{7.34}$$

Thus we determine the user's ray-centred coordinates of the point S situated on the paraxial ray by simple matrix multiplication. In addition, we obtain also the user's ray-centred components of the slowness vector at S.

Let us now consider a more complex situation: the initial point 0 of the paraxial ray is not, in general, situated in the plane perpendicular to Ω at 0_0, but it is close to 0_0. Moreover, its position is specified in the general coordinates $x^i(0)$. The initial slowness vector $\boldsymbol{p}(0)$ is specified by its covariant components $p_i(0)$ in the general coordinate system. We assume that both $x^i(0)$ and $p_i(0)$ are selected in such a way that the whole paraxial ray is situated close to the central ray Ω. We wish to determine the analytic equation for the paraxial ray in the vicinity of the point 0_s. We denote a point situated on the paraxial ray close to 0_s by S, and $x^i(S, 0_s) = x^i(S) - x^i(0_s)$. Then we obtain the following parametric equation for $x^i(S, 0_s)$:

$$x^i(S, 0_s) = G^{ik}(0_s)H_{kn}(0_s)q^n(S), \tag{7.35}$$

where q^3 is a (small) free parameter, and $q^1(S)$ and $q^2(S)$ are given by

$$q^K(S) = (Q_2(0_s, 0_0))_{KL} H_{mL}(0_0) G^{mn}(0_0) \times \{p_n(0) - p_n(0_0) - N_{nj}(0_0, 0_s) x^j(0, 0_0)\}. \tag{7.36}$$

The parametric equation (7.35) with (7.36) represents a straight-line approximation of the paraxial ray in the vicinity of the point 0_s. All the symbols in (7.36) have the same meaning as in (7.30) in Section 7.10.

It is simple to see that the point S is situated in the plane perpendicular to Ω at 0_s for $q^3 = 0$. For $q^3 > 0$ it is shifted "behind" this plane, and for $q^3 < 0$ "in front of" the plane.

7.12 Two-point ray tracing for paraxial rays

Assume that we know the position of the points 0 and S and we wish to find the ray that passes through these two points. This is the classical two-point ray-tracing problem. For paraxial rays this problem can be solved analytically. This means that we can find analytically approximate expressions for the slowness vector $\boldsymbol{p}(0)$ and/or $\boldsymbol{p}(S)$. The slowness vector determines the initial direction of the ray.

We again denote the general coordinates of S and 0 by $x^i(S)$ and $x^i(0)$ and use the notation (7.28). Differentiating (7.30), we obtain

$$\left.\begin{aligned} p_j(0) &= p_j(0_0) + N_{jk}(0_0, 0_s) x^k(0, 0_0) \\ &\quad + H_{jK}(0_0)(Q_2^{-1}(0_s, 0_0))_{KL} H_{mL}(0_s) x^m(S, 0_s), \\ p_j(S) &= p_j(0_s) + N_{jk}(0_s, 0_0) x^k(S, 0_s) \\ &\quad + H_{jK}(0_s)(Q_2^{-1}(0_s, 0_0))_{LK} H_{mL}(0_0) x^m(0, 0_0). \end{aligned}\right\} \tag{7.37}$$

All the symbols in (7.37) have the same meanings as in Section 7.10.

The solution (7.37) of the two-point ray-tracing problem is only approximate. The accuracy is, of course, higher for paraxial rays situated closer to the central ray Ω. The solution, however, can be repeated iteratively. An iterative loop in which the initial slowness vector at 0 is changed at each step can be used to find the ray that passes through the point S with the required accuracy.

7.13 Fresnel volumes

Fresnel volumes represent some vicinity of the central ray Ω that actually influences the wavefield at the receiver point 0_s. The Fresnel volumes are sometimes called the "*physical rays*" (see Kravtsov and Orlov, 1980). Let

us again assume that a point source is situated at 0_0 and the receiver at 0_s. Then the Fresnel volume is composed of points C for which the following condition holds:

$$|\tau(C, 0_0) + \tau(0_s, C) - \tau(0_s, 0_0)| < \tfrac{1}{2}T. \tag{7.38}$$

Here T is the period of the harmonic wave under consideration.

The Fresnel volume can be simply computed approximately by some algebraic manipulation with the propagator matrices. Let us consider a point 0_F situated on the ray Ω between 0_0 and 0_s. Any point F in the vicinity of the point 0_F is situated in the Fresnel volume if and only if

$$|[x^j(F) - x^j(0_F)]H_{jM}(0_F)[M_{MN}(0_F, 0_0) - M_{MN}(0_F, 0_s)]H_{kN}(0_F)[x^k(F) - x^k(0_F)]| < T. \tag{7.39}$$

Here the matrices

$$\boldsymbol{M}(0_F, 0_0) = \boldsymbol{P}_2(0_F, 0_0)(\boldsymbol{Q}_2(0_F, 0_0))^{-1} \tag{7.40a}$$

and

$$\boldsymbol{M}(0_F, 0_s) = [-\boldsymbol{P}_1(0_F, 0_0)\boldsymbol{Q}_2^{\mathrm{T}}(0_s, 0_0) + \boldsymbol{P}_2(0_F, 0_0)\boldsymbol{Q}_1^{\mathrm{T}}(0_s, 0_0)] \times [-\boldsymbol{Q}_1(0_F, 0_0)\boldsymbol{Q}_2^{\mathrm{T}}(0_s, 0_0) + \boldsymbol{Q}_2(0_F, 0_0)\boldsymbol{Q}_1^{\mathrm{T}}(0_s, 0_0)]^{-1}, \tag{7.40b}$$

are composed of the 2×2 submatrices of the ray propagator matrices

$$\boldsymbol{\Pi}(0_F, 0_0) = \begin{bmatrix} \boldsymbol{Q}_1(0_F, 0_0) & \boldsymbol{Q}_2(0_F, 0_0) \\ \boldsymbol{P}_1(0_F, 0_0) & \boldsymbol{P}_2(0_F, 0_0) \end{bmatrix} \tag{7.41}$$

and $\boldsymbol{\Pi}(0_s, 0_0)$ (see (7.11)). Both the matrices $\boldsymbol{\Pi}(0_F, 0_0)$ and $\boldsymbol{\Pi}(0_s, 0_0)$ are obtained by complete ray tracing along Ω from 0_0 to 0_s, passing through 0_F.

Equation (7.39) can be modified in many ways. Similar equations can be found for a point 0_F situated at a curved interface Σ. The intersection of the Fresnel volume with Σ will usually be represented by an ellipse. Only the part of the interface inside the ellipse will influence the wavefield at 0_s considerably.

7.14 Phase shift due to caustics. KMAH index

To evaluate the complex-valued amplitude of the displacement vector of the seismic body wave under consideration, it is necessary to take into account the phase shift due to caustics. In the algorithm for complete ray tracing proposed here the amplitudes are *automatically* modified by the relevant phase shift at any caustic point (see Section 5.8.3f). It may,

however, still be of some interest to know the complete phase shift $\delta\tau(0_s, 0_0)$ due to caustic points along Ω between 0_0 and 0_s. The phase shift $\delta\tau(0_s, 0_0)$ can be expressed in terms of the index $k(0_s, 0_0)$ of the ray trajectory Ω between 0_0 and 0_s by

$$\delta\tau(0_s, 0_0) = -\tfrac{1}{2}\pi k(0_s, 0_0). \tag{7.42}$$

The *index of the ray trajectory* $k(0_s, 0_0)$, also known as the *KMAH index*, is defined as the sum of the caustic points along Ω between 0_0 and 0_s; caustic points of second order (point caustics) being considered twice in this sum. We recall that $\det \boldsymbol{Q}^{\mathrm{R}} = 0$, $\boldsymbol{Q}^{\mathrm{R}} \neq \boldsymbol{0}$ at a caustic point of first order (simple caustic), and that $\boldsymbol{Q}^{\mathrm{R}} = \boldsymbol{0}$ at a caustic point of second order (point caustic). Here $\boldsymbol{Q}^{\mathrm{R}}$ is the matrix of geometrical spreading $\boldsymbol{Q}$ corresponding to the initial conditions (7.16) and (7.17). In the proposed procedure the KMAH index is stored in IY(12).

Note that the phase shift due to caustics is the only quantity evaluated in complete ray tracing that depends on the initial matrices $\boldsymbol{Q}^{\mathrm{INIT}}$ and $\boldsymbol{P}^{\mathrm{INIT}}$ (see Section 5.8.3f).

The existence, position, type and number of caustic points, and consequently the KMAH index, are changed if $\boldsymbol{Q}^{\mathrm{INIT}}$ and $\boldsymbol{P}^{\mathrm{INIT}}$ are changed.

7.15 Ray amplitudes

In the algorithm for complete ray tracing the vectorial complex-valued *reduced* amplitudes $A_i(0_s)$ given by (5.19) are evaluated at 0_s. They are expressed in the ray-centred coordinate system at 0_s. For convenience, the 3×3 matrix $\hat{\boldsymbol{A}}(0_s)$ is considered in this section. The element $A_{ij}(0_s)$ represents the ray-centred component in the direction of $\boldsymbol{e}_i(0_s)$ of the vectorial complex-valued *reduced* amplitude at 0_s corresponding to the unit initial vectorial complex-valued reduced amplitude at 0_0, polarized in the direction of $\boldsymbol{e}_j(0_0)$ (intrinsic choice). The non-zero quantities $\mathrm{Re}\,(A_{ij}(0_s))$ and $\mathrm{Im}\,(A_{ij}(0_s))$ are stored in Y(28), . . . , Y(27 + NAMPL), where NAMPL = 2, 4 or 8, depending on the type of the wave at 0_0 and 0_s (see Section 5.2.1).

The matrix A_{ij} is constructed from the stored quantities Y(28), . . . , Y(NY), with NY = NAMPL + 27, in the following way:

(a) P wave at the initial point of the ray 0_0, P wave at the point 0_s (NAMPL = 2):

$$A_{ij} = \begin{bmatrix} 0 & 0 & 0 \\ 0 & 0 & 0 \\ 0 & 0 & \mathrm{Y}(28) + \mathrm{iY}(29) \end{bmatrix};$$

(b) P wave at the initial point of the ray 0_0, S wave at the point 0_s (NAMPL = 4):

$$A_{ij} = \begin{bmatrix} 0 & 0 & Y(28) + iY(29) \\ 0 & 0 & Y(30) + iY(31) \\ 0 & 0 & 0 \end{bmatrix};$$

(c) S wave at the initial point of the ray 0_0, P wave at the point 0_s (NAMPL = 4):

$$A_{ij} = \begin{bmatrix} 0 & 0 & 0 \\ 0 & 0 & 0 \\ Y(28) + iY(29) & Y(30) + iY(31) & 0 \end{bmatrix};$$

(d) S wave at the initial point of the ray 0_0, S wave at the point 0_s (NAMPL = 8):

$$A_{ij} = \begin{bmatrix} Y(28) + iY(29) & Y(32) + iY(33) & 0 \\ Y(30) + iY(31) & Y(34) + iY(35) & 0 \\ 0 & 0 & 0 \end{bmatrix}.$$

We denote by $U^j(0_s)$ the contravariant components of the non-reduced complex-valued ray amplitude in the *local recording coordinate system* z^m *at* 0_s. If the local recording coordinate system z^m is Cartesian then we need not distinguish between covariant and contravariant components of the ray amplitudes. The local recording coordinate system may, of course, coincide with the general coordinate system, the user's ray-centred coordinate system, etc. We shall specify the local recording coordinate system z^m in terms of the 3×3 transformation matrix:

$$Z_k{}^j(0_s) = \frac{\partial z^j}{\partial x^k}(0_s), \qquad Z^j{}_k(0_s) = \frac{\partial x^j}{\partial z^k}(0_s). \tag{7.43}$$

Likewise, we introduce the contravariant components $U^j(0_0)$ of the ray amplitude with respect to the local coordinate system z^j at the initial point 0_0 of the ray, and the relevant transformation matrix:

$$Z^k{}_j(0_0) = \frac{\partial x^k}{\partial z^j}(0_0), \qquad Z_k{}^j(0_0) = \frac{\partial z^j}{\partial x^k}(0_0). \tag{7.44}$$

The local coordinates at the initial point 0_0 and the local recording coordinates at 0_s need not be of the same type.

The complex-valued vectorial ray amplitude (including the phase shift due to caustics) at 0_s is given by

$$U^j(0_s) = \left[\frac{v(0_0)\rho(0_0)}{v(0_s)\rho(0_s)}\right]^{1/2} (J(0_s))^{-1/2} C^j{}_n(0_s, 0_0) a^n(0_0), \tag{7.45}$$

where

$$C^j{}_n(0_s, 0_0) = Z_k{}^j(0_s)G^{km}(0_s)H_{mu}(0_s)A_{ur}(0_s, 0_0)H_{sr}(0_0)Z^s{}_n(0_0), \quad (7.46)$$

$$a^n(0_0) = \lim_{0 \to 0_0} \{(J(0))^{1/2}U^n(0)\}. \quad (7.47)$$

The path for the evaluation of the limit is along the ray, against the direction of propagation. The geometrical spreading $J = |\det \boldsymbol{Q}|$ is defined in Section 7.7.

For a *point source* at 0_0, (7.45) can be simplified. We can write

$$(J(0_s))^{-1/2}a^n(0_0) = |\det \boldsymbol{Q}_2(0_s, 0_0)|^{-1/2}v(0_0)g^n(0_0), \quad (7.48)$$

where

$$g^n(0_0) = \lim_{0 \to 0_0} \{(q^3(0) - q^3(0_0))U^n(0)\} \quad (7.49)$$

is the *radiation pattern of the point source.* The path for the evaluation of the limit is the same as in the case of (7.47). Thus, for a point source at 0_0, we can write

$$U^j(0_s) = v(0_0)\left[\frac{v(0_0)\rho(0_0)}{v(0_s)\rho(0_s)}\right]^{1/2} |\det \boldsymbol{Q}_2(0_s, 0_0)|^{-1/2}C^j{}_n(0_s, 0_0)g^n(0_0). \quad (7.50)$$

The radiation pattern $g^n(0_0)$ is, of course, a function of the ray parameters γ^1 and γ^2: $g^n = g^n(0_0, \gamma^1, \gamma^2)$.

7.16 Paraxial ray approximation for the ray amplitudes

Owing to the curvature of the wavefront, the direction of the slowness vector changes in the neighbourhood of the ray Ω. As the displacement vector is parallel to the slowness vector for P waves, and perpendicular to it for S waves, the vectorial complex-valued amplitudes also vary in the vicinity of Ω. Let us consider a point S close to 0_s. Then we can write approximately

$$U^j(S) = Z_k{}^j(S)G^{km}(0_s)H_{mn}(0_s)B_{nr}(S, 0_s)H_{sr}(0_s)Z^s{}_t(0_s)U^t(0_s). \quad (7.51)$$

Here $B_{nr}(S, 0_s)$ are elements of the 3×3 *paraxial approximation matrix* $\hat{\boldsymbol{B}}(S, 0_s)$. This matrix can be evaluated from the quantities obtained by the complete ray tracing. It is given by

$$\hat{\boldsymbol{B}}(S, 0_s) = \begin{bmatrix} 1 & 0 & \theta_1(S, 0_s) \\ 0 & 1 & \theta_2(S, 0_s) \\ -\theta_1(S, 0_s) & -\theta_2(S, 0_s) & 1 \end{bmatrix}. \quad (7.52)$$

Here $\theta_i(S, 0_s)$ are components of a 3×1 column matrix $\hat{\boldsymbol{\theta}}(S, 0_s)$:

$$\theta_i(S, 0_s) = v(0_s)H_{ki}(0_s)G^{kl}(0_s)N_{ln}(0_s)x^n(S, 0_s), \tag{7.53}$$

where $N_{ln}(0_s)$ is given by (7.25). Equation (7.52) may also be written in the form

$$B_{ij}(S, 0_s) = \delta_{ij} + v(0_s)[H_{ki}(0_s)\delta_{j3} - H_{kj}(0_s)\delta_{i3}]G^{kl}(0_s)N_{ln}(0_s)x^n(S, 0_s). \tag{7.54}$$

7.17 Amplitudes at structural interfaces or on the Earth's surface

If the point 0_s is situated at the structural interface then the above expressions for the ray amplitudes must be modified. Together with the incident wave, there are also two reflected waves (reflected P, reflected S) and two transmitted waves (transmitted P, transmitted S). Thus, to compute the amplitudes at 0_s, not only the quantities corresponding to the incident wave, but also those corresponding to the two reflected waves or two transmitted waves, must be stored.

Such a possibility is considered in the algorithm for complete ray tracing proposed here (see Section 5.5.4).

Let us assume that the quantities corresponding to the incident, reflected P and reflected S waves are stored at the point 0_s. We denote the quantities corresponding to the incident wave, to the reflected P wave and to the reflected S wave at 0_s by the superscripts IW, RP and RS respectively. We now denote by $\hat{\boldsymbol{U}}^{\mathrm{IW}}(0_s)$, $\hat{\boldsymbol{U}}^{\mathrm{RP}}(0_s)$ and $\hat{\boldsymbol{U}}^{\mathrm{RS}}(0_s)$ the 3×1 column matrices of the components of the ray amplitudes at 0_s, expressed in local recording or general coordinates, corresponding to the three waves under consideration. Then we can write

$$\hat{\boldsymbol{U}}(0_s) = \hat{\boldsymbol{U}}^{\mathrm{IW}}(0_s) + \hat{\boldsymbol{U}}^{\mathrm{RP}}(0_s) + \hat{\boldsymbol{U}}^{\mathrm{RS}}(0_s). \tag{7.55}$$

On the opposite side of the interface,

$$\hat{\boldsymbol{U}}(0_s) = \hat{\boldsymbol{U}}^{\mathrm{TP}}(0_s) + \hat{\boldsymbol{U}}^{\mathrm{TS}}(0_s), \tag{7.56}$$

where TP and TS correspond to the transmitted P and S waves.

If the point 0_s is situated on the Earth's surface then it is also possible to use, instead of (7.55), standard conversion coefficients (see Červený *et al.*, 1977). Such a possiblility is also optionally considered in the proposed algorithm (see Section 5.5.4). Equations (7.55) or (7.56) are, however, fully general and applicable at any interface, not only on the Earth's surface.

7.18 Ray amplitudes in slightly dissipative media

The quantities computed by complete ray tracing can be used to evaluate the amplitudes of seismic body waves in slightly dissipative media, for both causal and non-causal absorption. For simplicity, we shall only work here in the frequency domain.

In slightly dissipative media we can consider a complex-valued velocity v_C with a small imaginary part, which is formally assumed to be of order ω^{-1} for $\omega \to \infty$ (the so-called Debye procedure). The imaginary part of the velocity is not considered in the evaluation of rays and geometrical spreading and in the computation of the reflection/transmission coefficients, but it leads to an amplitude decay factor,

$$A_d(0_s) = \exp\left[-\omega \int_{0_0}^{0_s} \mathrm{Im}\left(\frac{1}{v_C(s)}\right) \mathrm{d}s\right], \tag{7.57}$$

where the integral is taken along the ray Ω from 0_0 to 0_s.

The amplitude decay factor $A_d(0_s)$ can be simply evaluated analytically for non-causal and various types of causal absorption if the quantity $t^* = 2Y(2)$ is known. This quantity, however, is evaluated by complete ray tracing. For *non-causal absorption* the amplitude decay factor is

$$A_d(0_s) = \exp(-\pi f t^*). \tag{7.58}$$

Similar equations for the amplitude decay factor for various *causal absorption* models (Futterman, Müller) can be found in Červený (1985a).

7.19 Displacement vector

In a perfectly elastic medium the contravariant components $u^j(0_s)$ of the displacement vector $\boldsymbol{u}(0_s)$ at the point 0_s are given by

$$u^j(0_s, \omega) = U^j(0_s) \exp[\mathrm{i}\omega\tau(0_s, 0_0)] \tag{7.59}$$

in the *frequency domain,* and by

$$u^j(0_s, t) = \mathrm{Re}\{U^j(0_s)\delta^{(A)}(t - \tau(0_s, 0_0))\} \tag{7.60}$$

in the *time domain.* Here ω is the circular frequency, $U^j(0_s)$ are given by (7.45) or (7.50), and $\tau(0_s, 0_0)$ by (7.1). The function $\delta^{(A)}(\xi)$ is the analytic unit impulse corresponding to the Dirac delta function $\delta(\xi)$: $\delta^{(A)}(\xi) = \delta(\xi) - \mathrm{i}/\pi\xi$. The time factor $\exp(-\mathrm{i}\omega t)$ in (7.59) is omitted. The time dependence at 0_0 in (7.60) is assumed here to be of the

form $\delta^{(A)}(t)$. The Fourier transform is assumed here to be of the form

$$\left.\begin{aligned} u^j(0_s, t) &= \frac{1}{\pi}\,\mathrm{Re}\int_0^\infty u^j(0_s, \omega)\mathrm{e}^{-\mathrm{i}\omega t}\,\mathrm{d}\omega, \\ u^j(0_s, \omega) &= \int_{-\infty}^{\infty} u^j(0_s, t)\mathrm{e}^{\mathrm{i}\omega t}\,\mathrm{d}t. \end{aligned}\right\} \tag{7.61}$$

Both expressions (7.59) and (7.60) can be simply modified to include effects of slightly dissipative media. For a non-causal absorption, this can be done using a complex-valued travel time $\tau(0_s, 0_0) + \frac{1}{2}\mathrm{i}t^*$ instead of the real-valued travel time $\tau(0_s, 0_0)$. The function $\delta^{(A)}(\xi)$ in (7.60) is then given by the relation

$$\delta^{(A)}(\xi) = -\frac{\mathrm{i}}{\pi\xi} = \mathrm{Im}\left(\frac{1}{\pi\xi}\right) - \mathrm{i}\,\mathrm{Re}\left(\frac{1}{\pi\xi}\right). \tag{7.62}$$

Let us now consider a real-valued source-time function $f(t)$ with a Fourier spectrum $F(\omega)$. Then, instead of (7.59) and (7.60), we obtain

$$u^j(0_s, \omega) = F(\omega)U^j(0_s)\exp\left[\mathrm{i}\omega\tau(0_s, 0_0)\right], \tag{7.63}$$

$$\begin{aligned} u^j(0_s, t) &= f(t) * \mathrm{Re}\left\{U^j(0_s)\delta^{(A)}(t - \tau(0_s, 0_0))\right\} \\ &= \mathrm{Re}\left\{f^{(A)}(t) * U^j(0_s)\delta(t - \tau(0_s, 0_0))\right\}. \end{aligned} \tag{7.64}$$

For absorbing media $\delta(\xi)$ is replaced by $\mathrm{Im}\,(1/\pi\xi)$. In (7.64), $f^{(A)}(t)$ denotes the complex-valued analytical signal corresponding to the real-valued function $f(t)$:

$$f^{(A)}(t) = \frac{1}{\pi}\int_0^\infty F(\omega)\mathrm{e}^{-\mathrm{i}\omega t}\,\mathrm{d}\omega = f(t) + \mathrm{i}g(t), \tag{7.65}$$

where $g(t)$ is the Hilbert transform of the function $f(t)$.

Expressions (7.59), (7.60), (7.63) and (7.64) correspond to the selected elementary wave propagating along the ray Ω from 0_0 to 0_s. In the time domain these expressions describe the so-called *elementary synthetic seismograms.*

7.20 Ray-synthetic body-wave seismograms

Until now, we have considered only one elementary wave specified by an appropriate alphanumeric code, and its ray passing through 0_s. In a layered medium, however, there may be many body waves that travel from the point source 0_0 or from the initial surface Σ to the point 0_s along various ray trajectories Ω. They correspond to various reflected, re-

fracted, multiply reflected, converted and other seismic body waves. Moreover, even a single elementary wave may travel to 0_s along different ray trajectories (so-called multiple rays). Thus for the complete high-frequency seismic body wavefield $\bar{u}^j$ at 0_s we can write the following *ray expansion*:

$$\bar{u}^j(0_s) = \sum_{(\Omega)} u^j(0_s), \tag{7.66}$$

where the summation runs over all rays Ω starting from 0_0 or from the initial surface Σ and passing through 0_s. The contributions $u^j(0_s)$ correspond to individual rays and are given by the equations of the previous section.

In a laterally varying layered structure the number of rays Ω arriving at 0_s may be infinite so that only a *partial-ray expansion* is actually possible. This, of course, introduces some errors into the ray computations.

In the *frequency domain* we can write

$$\bar{u}^j(0_s, \omega) = F(\omega) \sum_{(\Omega)} U^j(0_s) \exp[i\omega\tau(0_s, 0_0)]. \tag{7.67}$$

Here $U^j(0_s)$ and $\tau(0_s, 0_0)$ correspond to the previously derived and discussed expressions. Equation (7.67) represents the *synthetic frequency response* for $F(\omega) = 1$. The so-called FFR (fast frequency response) algorithm can be used to evaluate the synthetic frequency response very efficiently (see Červený, 1985c).

In the *time domain* the HF synthetic body-wave seismogram is obtained by the Fourier transform of (7.67) (see (7.61)):

$$\bar{u}^j(0_s, t) = \frac{1}{\pi} \mathrm{Re} \int_0^\infty \bar{u}^j(0_s, \omega) e^{-i\omega t} \, d\omega. \tag{7.68a}$$

Alternatively, we can write for the HF synthetic body-wave seismogram the expression

$$\begin{aligned} \bar{u}^j(0_s, t) &= f(t) * \mathrm{Re} \sum_{(\Omega)} U^j(0_s) \delta^{(A)}(t - \tau(0_s, 0_0)) \\ &= \mathrm{Re} \left\{ f^{(A)}(t) * \sum_{(\Omega)} U^j(0_s) \delta(t - \tau(0_s, 0_0)) \right\}. \end{aligned} \tag{7.68b}$$

Both of these expressions can be used even for complex-valued $\tau(0_s, 0_0)$ (dissipative media). $\delta^{(A)}(\xi)$ is then given by (7.62); $\delta(\xi)$ should be interpreted as $\mathrm{Im}\,(1/\pi\xi)$. The sum $\sum_{(\Omega)} \ldots$ in the second expression of (7.68b) represents the complex-valued *synthetic impulse response*.

For more details on ray-synthetic seismograms see the review by Červený (1985c).

7.21 Ray-theory elastodynamic Green function

We define the elastodynamic Green function $\bar{G}^m{}_n(0_s, t; 0_0, t_0)$ as follows: $\bar{G}^m{}_n(0_s, t; 0_0, t_0)$ is the mth contravariant component of the displacement vector in the local recording coordinate system at 0_s at time t, due to the application of a *single-force unit impulse* in the direction of the nth axis of the local initial coordinate system at 0_0 and time t_0. We can write approximately

$$\bar{G}^m{}_n(0_s, t; 0_0, t_0) = \sum_{(\Omega)} G^m{}_n(0_s, t; 0_0, t_0). \tag{7.69}$$

Here $G^m{}_n$ are the contributions corresponding to rays Ω of individual elementary waves (including multiple arrivals).

To determine $G^m{}_n$, we use (7.50) and specify the radiation pattern $g^j(0_0)$ for the single force oriented along the nth axis of the local initial coordinate system. We obtain (see Kennett, 1983),

$$g^j(0_0) = \begin{cases} (4\pi\rho(0_0)v^2(0_0))^{-1} & \text{for } j = n, \\ 0 & \text{for } j \neq n. \end{cases}$$

In the *time domain* this yields

$$G^m{}_n(0_s, t; 0_0, t_0) = A(0_s, 0_0)\,\mathrm{Re}\,\{C^m{}_n(0_s, 0_0)\delta^{(A)}(t - t_0 - \tau(0_s, 0_0))\}, \tag{7.70}$$

where

$$A(0_s, 0_0) = \frac{1}{4\pi}[v(0_0)\rho(0_0)v(0_s)\rho(0_s)\,|\det \boldsymbol{Q}_2(0_s, 0_0)|]^{-1/2}. \tag{7.71}$$

In the *frequency domain* we have

$$G^m{}_n(0_s, 0_0, \omega) = A(0_s, 0_0)C^m{}_n(0_s, 0_0)\exp(\mathrm{i}\omega\tau(0_s, 0_0)), \tag{7.72}$$

where $G^m{}_n(0_s, 0_0, \omega)$ denotes the Fourier spectrum of $G^m{}_n(0_s, t; 0_0, 0)$.

7.22 Moment-tensor point source

Using the Green function, we can easily write expressions for point sources of more general types in 3D laterally varying layered block structures. Let us denote the contravariant components of the moment tensor by $M^{kl}(t)$. Then the contravariant components $\bar{u}^n(0_s, t)$ of the displacement vector at 0_s are given by

$$\bar{u}^n(0_s, t) = \dot{M}^{ij}(t) * \sum_{(\Omega)} G^n{}_i(0_s, t; 0_0, 0)p_j(0_0). \tag{7.73}$$

Here $\dot{M}^{ij}(t)$ denotes the time derivatives of the moment tensor and $p_j(0_0)$ are covariant components of the slowness vector at the source point 0_0. This equation can be rewritten in many alternative forms; one of which is

$$\bar{u}^n(0_s, t) = \mathrm{Re}\left\{(\dot{M}^{ij}(t))^{(A)} * \sum_{(\Omega)} A(0_s, 0_0) \times C^n{}_i(0_s, 0_0) p_j(0_0) \delta(t - t_0 - \tau(0_s, 0_0))\right\}. \quad (7.74)$$

Here $(\dot{M}^{ij}(t))^{(A)}$ denotes the analytical signal corresponding to the time derivative of $M^{ij}(t)$, $A(0_s, 0_0)$ is given by (7.71) and $C^n{}_i(0_s, 0_0)$ by (7.46).

The ray method can only be used to compute the high-frequency part of the seismic wavefield. Thus the resulting seismograms must be high-pass filtered to exclude the low-frequency contributions if such contributions are included in the source-time function.

7.23 Particle-motion diagrams

As the local recording coordinate system z^n at 0_s can be chosen arbitrarily by the user, complete ray tracing offers the possibility of determining and plotting particle-motion diagrams in an arbitrary plane passing through 0_s. The particle-motion diagrams of the complete wavefield may, in general, be rather complicated, mainly in various interference regions of two or more elementary waves, even in the ray approximation. The particle-motion diagrams considerably simplify for individual elementary waves if they are separated from other waves. For simplicity, let us consider harmonic waves, and a point 0_s situated inside the medium. When the wave arrives at 0_s as a P wave it is linearly polarized at that point. When the wave arrives at 0_s as an S wave its polarization is more complicated: as a rule, the S wave is elliptically polarized. The elliptical polarization may be caused by radiation patterns of the source and by overcritical reflections at interfaces. If the point 0_s is situated at an interface then the polarization may be elliptical for both the incident P and S waves, as both waves may impinge at the interface overcritically. Finally, at the Earth's surface, the polarization remains linear for the incident P wave (the P wave always impinges subcritically at the surface). The S wave, however, very often impinges overcritically at the Earth's surface. In this case its polarization is elliptical at 0_s even if the incident S wave is polarized linearly.

7.24 Gaussian beams and Gaussian packets

Expressions for the displacement vector (7.63) and (7.64) are high-frequency solutions of the elastodynamic equation even if the real-valued solutions $\boldsymbol{Q}$, $\boldsymbol{P}$ and $\boldsymbol{M}$ of the dynamic ray-tracing system are replaced by complex-valued solutions of that system. For positive-definite Im $\boldsymbol{M}$ such a solution represents a *Gaussian beam* concentrated near the ray Ω. The amplitude profile of the Gaussian beam in the plane perpendicular to the ray Ω is Gaussian, with its maximum on the ray Ω. The matrix $\boldsymbol{L} = (\frac{1}{2}\omega \operatorname{Im} \boldsymbol{M})^{-1/2}$ represents the matrix of the halfwidth of the Gaussian beam.

If the matrices Re $\boldsymbol{M}(0_0)$ and Im $\boldsymbol{M}(0_0)$ (or $\boldsymbol{L}(0_0)$) are given at the initial point 0_0 of the ray Ω, the matrices Re $\boldsymbol{M}(0_s)$, Im $\boldsymbol{M}(0_s)$ (and $\boldsymbol{L}(0_s)$) can be simply determined at any point 0_s of the ray Ω, using the results of complete ray tracing (particularly the ray propagator matrix $\boldsymbol{\Pi}(0_s, 0_0)$) and (7.22).

Similarly, if $\boldsymbol{Q}(0_0)$ and $\boldsymbol{P}(0_0)$ are given then Re $\boldsymbol{Q}(0_s)$ and Im $\boldsymbol{Q}(0_s)$ may be determined by means of the propagator matrix $\boldsymbol{\Pi}(0_s, 0_0)$ and (7.14). To apply (7.63) and (7.64) to the computation of Gaussian beams, the geometrical spreading $|\det \boldsymbol{Q}(0_s)|^{-1/2}$ must be replaced by $[\det \boldsymbol{Q}(0_s)]^{-1/2}$ and the phase shift due to caustics must be removed from the amplitude factor. As the KMAH index is known, the phase shift due to caustics can be removed simply. The sign of $[\det \boldsymbol{Q}(0_s)]^{-1/2}$, however, is not determined by complete ray tracing. Thus we can use complete ray tracing to obtain the final expressions for the displacement vector of the single Gaussian beam concentrated near Ω at 0_s, *except for the sign*. If the phase shift due to caustics is not removed then the ambiguous multiplicative factor is i^n ($n = 0, 1, 2, \ldots$).

In some applications of Gaussian beams—for example in the computation of the wavefield by the *summation* of Gaussian beams—the ambiguous multiplicative factor need not be known, it is cancelled by other factors in the summation formulae. Thus complete ray tracing is quite suitable for determining the Gaussian-beam contributions for the summation procedures.

As for Gaussian beams, the results of complete ray tracing can be used to compute the Gaussian packets (also called "quasiphotons"; see Babich and Ulin, 1981) concentrated near points along Ω, again except for the abovementioned ambiguous multiplicative factor. The amplitudes of the Gaussian packet concentrated near a point 0_s of the ray Ω decay exponentially with the square of the distance from 0_s, not only in the direction perpendicular to Ω, but in all directions.

If the results of complete ray tracing are stored in a sufficiently dense

system of points along Ω between 0_0 and 0_s then the ambiguity factor can be removed, as $[\det \boldsymbol{Q}]^{-1/2}$ must vary continuously and smoothly along Ω in the case of Gaussian beams, even through caustic points.

For more details regarding Gaussian beams and Gaussian packets see the reviews by Červený (1985a,b) and references cited therein.

7.25 Summation of Gaussian beams or Gaussian packets

A time-harmonic high-frequency seismic body wavefield can be approximately expressed by a summation of Gaussian beams. For each elementary wave composing the wavefield, a sufficiently dense two-parameter system of rays is evaluated by the standard complete ray tracing. The wavefield can be expanded into a two-parameter system of Gaussian beams concentrated near individual rays. The final wavefield at any receiving point is then obtained by summation of all beams passing in some vicinity of the receiver. The Gaussian beams far from the receiver need not be considered in the summation owing to the finite width of the beam. For details and for the expansion formulae see Klimeš (1984a, 1986) and Červený (1985a).

In a similar way, the wavefield can be asymptotically expressed by summation of a three-parameter system of Gaussian packets. For each ray of the abovementioned two-parameter system of rays, a system of Gaussian packets concentrated near regularly distributed points along the ray is constructed. The summation is over all Gaussian packets influencing the wavefield at the receiver. As in the case of Gaussian beams, the Gaussian packets concentrated near points far from the receiver need not be considered. For details see Klimeš (1984b).

In the summation formulae, infinitely broad Gaussian beams (paraxial ray approximations) can be used instead of Gaussian beams of finite width. In this way, the Maslov method (see Chapman and Drummond, 1982; Klimeš, 1984b; Thompson and Chapman, 1985) may be obtained.

In 2D computations it is not necessary to evaluate a two-parameter system of rays—a one-parameter system of rays is sufficient. Two-dimensional (ribbon) Gaussian beams must, however, be used in the summation formulae. See Červený and Pšenčík (1983a) and Červený (1985a).

A similar simplified procedure based on the summation of Gaussian beams can be used even in 3D media if we are interested in the wavefield only along a specified profile (generally curvilinear). In such a case the tracing of only those rays that approximately follow the profile is

sufficient. The take-off parameters of these rays form a curve in the 2D set of ray parameters γ^1 and γ^2. Such a computation is called the *profile mode computation* here.

In this case the quantity YI(22) = Γ (see (6.1)) must be replaced by the arclength of that part of the abovementioned curve in the ray-parameter surface that corresponds to the ray under consideration. The matrix Γ_{KL} (see (6.2)) is then singular, with one zero eigenvalue. The eigenvector corresponding to the non-zero eigenvalue is tangential to the curve in the ray-parameter surface; the other one is perpendicular to the curve. However, the algorithm for complete ray tracing remains the same.

Profile-mode computation in 3D media is *numerically very efficient*; it is only slightly more time-consuming than standard 2D computations. It may be used in the numerical modelling of high-frequency seismic wavefields in various source–receiver configurations: for surface profiles (in deep seismic sounding of the lithosphere, etc.), for borehole profiles (vertical seismic profiling), for borehole-to-borehole computations, in normal ray section computations, etc.

7.26 Integrals of the ray propagator matrix along the ray

Some integrals of the type

$$B_\beta = \int_{\sigma_0}^{\sigma} F_\alpha(\sigma) \Pi_{\alpha\beta}(\sigma, \sigma_0)\, \mathrm{d}\sigma \tag{7.75}$$

or

$$B_{\alpha\beta} = \int_{\sigma_0}^{\sigma} \Pi_{\gamma\alpha}(\sigma, \sigma_0) F_{\gamma\delta}(\sigma) \Pi_{\delta\beta}(\sigma, \sigma_0)\, \mathrm{d}\sigma, \tag{7.76}$$

where the quadrature is performed along the ray Ω and σ is defined by (5.1), are important in *perturbation theory* (Farra and Madariaga, 1987) and in *optimization of the shape of Gaussian beams and packets* (Klimeš, 1985). Here the weighting functions $F_\alpha(\sigma)$ and $F_{\gamma\delta}(\sigma)$ along the ray may be dependent on the velocities and their derivatives and/or on the velocity perturbations. $\sigma = \sigma_0$ denotes the initial point of the ray Ω.

There are two ways of evaluating the integrals.

(a) The numerical quadratures may be substituted directly into the complete ray-tracing algorithm. This approach has two disadvantages: (i) the complete ray-tracing algorithm is more complicated;

(ii) the integrals are only evaluated for the previously specified weighting functions and the weighting functions cannot be changed without repeating the complete ray-tracing computations.

(b) The results of complete ray tracing are stored along the ray Ω with the step STORE (see Section 5.5.1) of the independent variable σ. Then the integrals may be computed later by means of another program. This approach has two disadvantages: (i) since the quantities are stored with a given step of an independent variable, the points of intersection of the ray with the interfaces must also be stored in a file and taken into account; (ii) since the weighting functions are usually dependent on the velocity distribution, the routine computing the velocity and its derivatives must be called again for each stored point of the ray if some unstored derivatives of velocity are required.

The matrix $B_{\alpha\beta}$ defined above is often ill-conditioned, even in the case of a well-conditioned positive-definite weighting matrix $F_{\alpha\beta}(\sigma)$. For this reason, it is recommended that rather than directly evaluating the matrix $B_{\alpha\beta}$, with

$$\boldsymbol{B} = \begin{bmatrix} \boldsymbol{B}_{11} & \boldsymbol{B}_{12} \\ \boldsymbol{B}_{21} & \boldsymbol{B}_{22} \end{bmatrix}, \tag{7.77}$$

one should evaluate the matrix (Klimeš, 1985)

$$\boldsymbol{C} = \begin{bmatrix} \boldsymbol{C}_{11} & \boldsymbol{C}_{12} \\ \boldsymbol{C}_{21} & \boldsymbol{C}_{22} \end{bmatrix} = \begin{bmatrix} \boldsymbol{B}_{11} - \boldsymbol{B}_{12}\boldsymbol{B}_{22}^{-1}\boldsymbol{B}_{21} & \boldsymbol{B}_{12} \\ \boldsymbol{B}_{21} & \boldsymbol{B}_{22} \end{bmatrix}. \tag{7.78}$$

The differential equations

$$\begin{aligned} \frac{\mathrm{d}}{\mathrm{d}\sigma}\boldsymbol{C}_{11} &= [\boldsymbol{\Pi}_1(\sigma, \sigma_0) - \boldsymbol{\Pi}_2(\sigma, \sigma_0)\boldsymbol{C}_{22}^{-1}\boldsymbol{C}_{21}]^{\mathrm{T}} \\ &\quad \times \boldsymbol{F}(\sigma)[\boldsymbol{\Pi}_1(\sigma, \sigma_0) - \boldsymbol{\Pi}_2(\sigma, \sigma_0)\boldsymbol{C}_{22}^{-1}\boldsymbol{C}_{21}], \\ \frac{\mathrm{d}}{\mathrm{d}\sigma}\boldsymbol{C}_{21} &= \boldsymbol{\Pi}_2^{\mathrm{T}}(\sigma, \sigma_0)\boldsymbol{F}(\sigma)\boldsymbol{\Pi}_1(\sigma, \sigma_0), \\ \frac{\mathrm{d}}{\mathrm{d}\sigma}\boldsymbol{C}_{12} &= \boldsymbol{\Pi}_1^{\mathrm{T}}(\sigma, \sigma_0)\boldsymbol{F}(\sigma)\boldsymbol{\Pi}_2(\sigma, \sigma_0), \\ \frac{\mathrm{d}}{\mathrm{d}\sigma}\boldsymbol{C}_{22} &= \boldsymbol{\Pi}_2^{\mathrm{T}}(\sigma, \sigma_0)\boldsymbol{F}(\sigma)\boldsymbol{\Pi}_2(\sigma, \sigma_0) \end{aligned} \tag{7.79}$$

for the 2×2 submatrices of $\boldsymbol{C}$ follow directly from (7.76). Here

$$\boldsymbol{\Pi}_1(\sigma, \sigma_0) = \begin{bmatrix} \boldsymbol{Q}_1(\sigma, \sigma_0) \\ \boldsymbol{P}_1(\sigma, \sigma_0) \end{bmatrix}, \qquad \boldsymbol{\Pi}_2(\sigma, \sigma_0) = \begin{bmatrix} \boldsymbol{Q}_2(\sigma, \sigma_0) \\ \boldsymbol{P}_2(\sigma, \sigma_0) \end{bmatrix}.$$

In (7.79), σ is again the variable along the ray Ω defined by (5.1).

7.27 Other applications

In principle, complete ray tracing can be effectively used in any sort of numerical modelling of high-frequency seismic wavefields in complex 2D and 3D structures, including the computation of the high-frequency seismic wavefield generated by finite sources (Červený *et al.*, 1987), the solution of various diffraction problems, the investigation of the effects of local geological conditions on surface motion, and the evaluation of Kirchhoff integrals, as well as those applications mentioned above. Similarly, complete ray tracing is sure to find applications in the solution of inverse seismic problems, both kinematic and dynamic. For example, Klimeš (1987) applied complete ray tracing and the Gaussian-packet approach in an algorithm for the kinematic location of hypocentres in general 3D models.

The number of applications of complete ray tracing is growing rapidly, and complete ray tracing is bound to play an important role in many other problems of seismological importance.

REFERENCES

Babich, V. M. and Ulin, V. V. (1981). Complex space-time ray method and "quasiphotons". *Mathematical Problems of the Theory of Wave Propagation* (ed. V. M. Babich), pp. 5–12. Nauka, Leningrad. (In Russian.)

Červený, V. (1985a). The application of ray tracing to the numerical modelling of seismic wave fields in complex structures. *Seismic Shear Waves,* Part A: *Theory* (ed. G. Dohr), pp. 1–124. Geophysical Press, London.

Červený, V. (1985b). Gaussian beam synthetic seismograms. *J. Geophys.* **58,** 44–72.

Červený, V. (1985c). Ray synthetic seismograms for complex two-dimensional and three-dimensional structures. *J. Geophys.* **58,** 2–26.

Červený, V. and Pšenčík, I. (1983a). Gaussian beams in two-dimensional elastic inhomogeneous media. *Geophys. J. R. Astron. Soc.* **72,** 419–435.

Červený, V. and Pšenčík, I. (1983b). Gaussian beams and paraxial ray approximations in three-dimensional elastic inhomogeneous media. *J. Geophys.* **53,** 1–15.

Červený, V., Molotkov, I. A. and Pšenčík, I. (1977). *Ray Method in Seismology.* Universita Karlova, Praha.

Červený, V., Klimeš, L. and Pšenčík, I. (1984). Paraxial ray approximations in the computation of seismic wave field in inhomogeneous media. *Geophys. J. R. Astron. Soc.* **79,** 89–104.

Červený, V., Klimeš, L., Pšenčík, I. and Pleinerová, J. (1987). High-frequency radiation from earthquake sources in laterally varying layered structures. *Geophys. J. R. Astron. Soc.* **88,** 43–79.

Chapman, C. H. and Drummond, R. (1982). Body wave seismograms in inhomogeneous media using Maslov asymptotic theory. *Bull. Seismol. Soc. Am.* **72,** S277–S317.

Farra, V. and Madariaga, R. (1987). Seismic waveform modelling in heterogeneous media by ray perturbation theory. *J. Geophys. Res.* **92,** 2697–2712.

Gjøystdal, H., Reinhardsen, J. E. and Astebøl, K. (1985). Computer representation of complex 3-D geological structures using a new "solid modeling" technique. *Geophys. Prosp.*, **33,** 1195–1211.

Kennett, B. L. N. (1983). *Seismic Wave Propagation in Stratified Media.* Cambridge University Press.

Klimeš, L. (1984a). Expansion of a high-frequency time-harmonic wave field given on an initial surface into Gaussian beams. *Geophys. J. R. Astron. Soc.* **79,** 105–118.

Klimeš, L. (1984b). The relation between Gaussian beams and Maslov asymptotic theory. *Stud. Geophys. Geod.* **28,** 237–247.

Klimeš, L. (1985). Computation of seismic wavefields in 3-D media by the Gaussian beam method. Program SW84. Research Report 68. Institute of Geophysics, Charles University, Praha. (In Czech.)

Klimeš, L. (1986). Discretization error for the superposition of Gaussian beams. *Geophys. J. R. Astron. Soc.* **86,** 531–551.

Klimeš, L. (1987). Kinematic hypocentre location. *Acta Montana* **75,** 51–64. (In Czech, English abstract.)

Kravtsov, Y. A. and Orlov, Y. I. (1980). *Geometrical Optics of Inhomogeneous Media.* Nauka, Moscow. (In Russian.)

Popov, M. M. and Pšenčík, I. (1978a). Ray amplitudes in inhomogeneous media with curved interfaces. *Travaux Géophysiques,* Vol. 24 (ed. A. Zátopek), pp. 118–129. Academia, Praha.

Popov, M. M. and Pšenčík, I. (1978b). Computation of ray amplitudes in inhomogeneous media with curved interfaces. *Stud. Geophys. Geod.* **22,** 248–258.

Thompson, C. J. and Chapman, C. H. (1985). An introduction to the Maslov asymptotic method. *Geophys. J. R. Astron. Soc.* **83,** 143–168.